Quaternary Science Reviews xxx (2012) 1–16

Contents lists available at SciVerse ScienceDirect

Quaternary Science Reviews

journal homepage: www.elsevier.com/locate/quascirev

Lithology, radiocarbon chronology and sedimentological interpretation of the lacustrine record from Laguna Potrok Aike, southern Patagonia

Pierre Kliem [a,*], Dirk Enters [a], Annette Hahn [a], Christian Ohlendorf [a], Agathe Lisé-Pronovost [b,c], Guillaume St-Onge [b,c], Stefan Wastegård [d], Bernd Zolitschka [a] and the PASADO science team [1]

[a] Geomorphology and Polar Research (GEOPOLAR), Institute of Geography, University of Bremen, Celsiusstr., FVG-M, D-28359 Bremen, Germany
[b] Institut des sciences de la mer de Rimouski (ISMER), Université du Québec à Rimouski (UQAR), Québec, Canada
[c] GEOTOP Research Center, Québec, Canada
[d] Dept. of Physical Geography and Quaternary Geology, Stockholm University, SE-106 91 Stockholm, Sweden

ARTICLE INFO

Article history:
Received 20 December 2011
Received in revised form
1 July 2012
Accepted 19 July 2012
Available online xxx

Keywords:
Mixed-effect regression
Mass movement deposits
Lake level fluctuations
Late Pleistocene
Holocene
Patagonia
Argentina
ICDP-project PASADO

ABSTRACT

The 106 m long composite profile from site 2 of ICDP expedition 5022 (PASADO) at Laguna Potrok Aike documents a distinct change in sedimentation patterns from pelagic sediments at the top to dominating mass movement deposits at its base. The main lithological units correspond to the Holocene, to the Lateglacial and to the last glacial period and can be interpreted as the result of distinct environmental variations. Overflow conditions might have been achieved during the last glacial period, while signs of desiccation are absent in the studied sediment record. Altogether, 58 radiocarbon dates were used to establish a consistent age-depth model by applying the mixed-effect regression procedure which results in a basal age of 51.2 cal. ka BP. Radiocarbon dates show a considerable increase in scatter with depth which is related to the high amount of reworking. Validation of the obtained chronology was achieved with geomagnetic relative paleointensity data and tephra correlation.

1. Introduction

Lacustrine sediments are often outstanding natural archives and complement marine and ice core records to reveal a consistent global picture of past environmental and climatic changes. However, terrestrial paleoclimatic data reaching far back into the Pleistocene are rare, especially from the Southern Hemisphere where southernmost South America is the only continental land mass between 40°S and 60°S. But here climate archives, mostly fen and lake sediments at the foot of the Andes, comprise only the past 18 cal. ka BP (Gilli et al., 2005; Markgraf et al., 2007; Wille and Schäbitz, 2009; Markgraf and Huber, 2010; Moy et al., 2011). Older records can only be found in extra-Andean Patagonia like at Laguna Potrok Aike, Patagonia (51°58′ S, 70°23′ W). This site emerged as a valuable terrestrial paleoclimate archive for the last 16 cal. ka BP (Zolitschka et al., 2006; Haberzettl et al., 2007; Anselmetti et al., 2009; Mayr et al., 2009), and the Potrok Aike Maar Lake Sediment Archive Drilling Project (PASADO) was established to extend the climate record back in time. Such a sediment archive would allow to investigate shifts in polar to mid-latitude pressure fields and precipitation changes related to the Southern Hemispheric Westerlies as well as the Antarctic Oscillation and allows inter-comparisons between paleodata and climate models (Wagner et al., 2007; Meyer and Wagner, 2008). Due to the location of Laguna Potrok Aike in the Patagonian steppe leeward of the Andean mountain range, it should also be suited to establish a tephra and dust record which may be linked to marine records and ice cores from Antarctica. Furthermore, the possible extension of the Patagonian tephrochronology beyond the Lateglacial will provide the needed chronological control for other investigations using terrestrial as well as marine records.

Especially for multidisciplinary projects like PASADO, the initial lithological core description is essential and gives an overview about the compositional variability of the sediment record

* Corresponding author.
E-mail address: kliem@uni-bremen.de (P. Kliem).
[1] PASADO Science Team as listed at http://www.icdp-online.org/front_content.php?idcatart=2794.

0277-3791/$ – see front matter © 2012 Elsevier Ltd. All rights reserved.
http://dx.doi.org/10.1016/j.quascirev.2012.07.019

(lithological units) and the occurrence of unconformities and bedding structures (Schnurrenberger et al., 2003). This information is important to adjust the sampling scheme and to omit reworked sediment units from further time-consuming and expensive analyses. Moreover and most important, the significance of the obtained paleoenvironmental information depends on a reliable age-depth model. Only if time control is available, a comparison with other records becomes possible and lithological changes can be quantified with variations in sedimentation rates. Thus, the objectives of this study are to (1) describe the lithological changes encountered along the sediment record, (2) establish a robust radiocarbon-based age-depth model and (3) interpret the observed sedimentological variability.

2. Site description

Laguna Potrok Aike is a polymictic and subsaline maar lake located in the Pali Aike Volcanic Field (PAVF) at 113 m a.s.l. (Fig. 1). It has a maximum diameter of 3.5 km and a water depth of 100 m with a volume of 0.41 km^3 (Zolitschka et al., 2006). According to the isotopic composition of the water body Laguna Potrok Aike is a groundwater lake (Mayr et al., 2007a). Rapid hydrological variations are documented by subaerial and subaqueous lake level terraces (Haberzettl et al., 2005; Anselmetti et al., 2009). At present the lake neither has a permanent tributary nor an outflow. A paleo-outflow related to a higher lake level is discussed for the Lateglacial (Haberzettl et al., 2007). Currently, only episodic or ephemeral surface runoff incised deep gullies in the surrounding subaerial terraces (Mayr et al., 2007a).

The PAVF is a region in the Province of Santa Cruz (Argentina) characterized by backarc volcanism (Mazzarini and D'Orazio, 2003). This intra-plate volcanism consists of Pliocene (3.8 Ma) to Holocene (0.01 Ma) alkali-olivine basalts (Corbella, 2002). The investigated maar itself is located in the older western part of the PAVF with scoria cones, plateau lavas and maar volcanoes occurring in the catchment area. A basaltic clast from the phreatomagmatic tephra of the maar eruption was dated by Ar/Ar and provides an age of 0.77 ± 0.24 Ma (Zolitschka et al., 2006). Outcrops of weakly compacted sandstone exist along the perimeter of the lake on subaerial terraces. These belong to Lower Miocene fine-grained molasse-type fluvial sandstones of the Santa Cruz Formation which is the youngest formation in the Magellanes Basin (Uliana and Biddle, 1988). Plio- and Pleistocene glaciations left behind fluvioglacial deposits and till in the catchment area, but glaciers did not reach the catchment area during the last few glaciations (Caldenius, 1932; Coronato et al., in this issue; Mercer, 1976; Rabassa and Clapperton, 1990; Meglioli, 1992).

Due to the proximity of the Antarctic continent, during austral summers the small land mass of southern Patagonia does not warm up as much as continents in the same latitude of the Northern Hemisphere (Weischet, 1996). The mean annual temperature at Rio Gallegos (6 m a.s.l., 85 km north-east of the study site) is only 7.4 ± 0.7 °C (Zolitschka et al., 2006). The regional climate is affected by the Southern Hemispheric Westerlies. The rain shadow effect of the north–south striking Andean mountain chain decreases precipitation to less than 300 mm (Mayr et al., 2007b). At the meteorological station next to Laguna Potrok Aike an annual precipitation sum of 150 mm has been observed (Zolitschka et al., 2006). Mean annual wind speeds of 7.4 m/s occur at Rio Gallegos; primarily from westerly directions (Weischet, 1996; Baruth et al., 1998). Recent series of precipitation measurements (1999–2005) at Laguna Potrok Aike reveal that easterly wind directions are often combined with precipitation whereas west winds do not carry considerable amounts of moisture into the area (Mayr et al., 2007b).

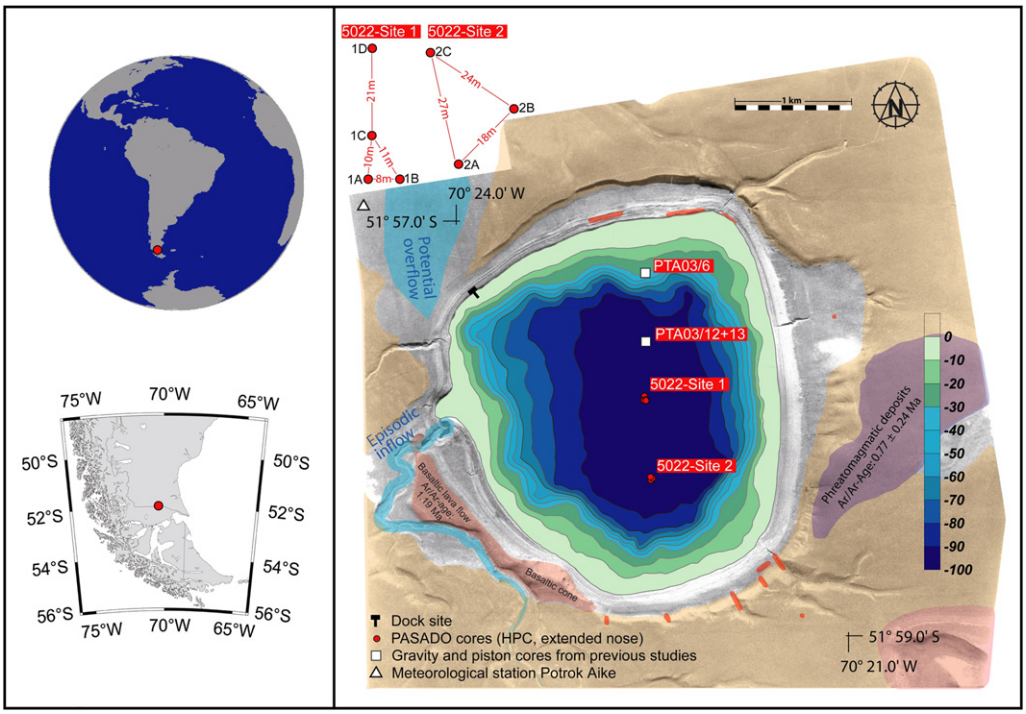

Fig. 1. Location of Laguna Potrok Aike in the southern hemisphere, in southern South America and bathymetric map with position of drill sites merged with an aerial photograph and geological data (Corbella, 2002; Zolitschka et al., 2006). Depth is given in m below lake surface. Young fluvial and lacustrine deposits (gray), a mid-Pleistocene basalt lava flow (red), phreatomagmatic tephra deposits (pink), moraine till (yellow), and the Tertiary Santa Cruz Formation (orange) are color-coded. (For interpretation of the references to color in this figure legend, the reader is referred to the web version of this article.)

Please cite this article in press as: Kliem, P., et al., Lithology, radiocarbon chronology and sedimentological interpretation of the lacustrine record from Laguna Potrok Aike, southern Patagonia, Quaternary Science Reviews (2012), http://dx.doi.org/10.1016/j.quascirev.2012.07.019

3. Field work and laboratory methods

From August to November 2008 the ICDP lake deep drilling expedition 5022 (PASADO) was carried out with the GLAD800, a containerized barge system equipped with a CS-1500 drill rig and operated by the non-profit organization DOSECC (Drilling, Observation and Sampling of the Earths Continental Crust). Hydraulic piston corer and extended nose devices were used as drill tools. Full core runs consisted of 2.92 m sediment sections in Butyrate liners (inner diameter: 66.34 mm) plus 8 cm sediment of the core catcher. At two drill sites a total of four (Site 1) and three (Site 2) overlapping core series have been recovered (Fig. 1). Liners were cut into 1.5 m sections on the drilling barge, then shuttled to the shore using a custom-built catamaran and finally stored in a cooling container in which they were shipped to the University of Bremen, Germany, for storage in the GEOPOLAR core repository at 4 °C.

Smear slides of core catcher sediment were prepared in the shore-based field laboratory according to Myrbo (2007) for the microscopic identification of sedimentary components such as carbonates or volcanogenic minerals.

A new protocol for sediment core treatment and subsampling for multiproxy analyses was developed for PASADO (Ohlendorf et al., 2011) and applied after plastic liners were cut lengthwise with a manual splitter at the laboratory of the University of Bremen. Depending on sediment consistency, core sections were split with sharpened plates made of phosphorous bronze, nylon wire or steel guitar strings. In a next step the sediment surface was cleaned and smoothed with a sharpened blade. Photographic images were taken from fresh surfaces using a digital camera image scanner (SmartCIS, Smartcube) with a resolution of 500 dpi. With this system individual 10 cm long images (jpg format) of the sediment are automatically stitched together into a composite of the complete core section. Core sections were described lithologically, using the categories rock class (sedimentary), rock type (siliciclastic, volcaniclastic, organic), grain size, structure, texture, components (gastropods, plant macro remains, animal bones) and color. Core descriptions were entered into the ICDP Drilling Information System (DIS) database (Conze et al., 2007) to make them available to the entire PASADO scientific community. Based on lithologic characterization and after macroscopic correlation of parallel cores from both sites, two composite profiles were assembled. Site 2 was established as the key site with the composite record 5022-2CP based on three parallel holes (Fig. 2) with a total recovery rate of 95.2%. Sections of undisturbed sediment and without gaps were selected to establish the chronostratigraphy for this composite profile.

Plant macro remains of aquatic mosses were sampled from 5022-2CP for radiocarbon dating. Samples were sieved through a 200 μm sieve, cleaned with demineralized water and dried at 60 °C before they were sent to the Poznan Radiocarbon Laboratory for AMS-^{14}C determination. The top 18 m of 5022-2CP were not sampled for radiocarbon dating. Instead, ^{14}C dates were transferred for this section from the profile PTA03/12 + 13 (Haberzettl et al., 2007) using lithological features and magnetic susceptibility data as means for correlation. The latter have been obtained from cling-film covered cores in 5 mm increments with a Bartington MS2F-sensor mounted on an automated scanner.

Calibration of all radiocarbon dates from 5022-2CP as well as re-calibration of the correlated dates from PTA03/12 + 13 was carried out with the CalPal_2007_HULU calibration dataset (Weninger and Jöris, 2008) and the download-version of the CalPal calibration software (Weninger et al., 2010). CalPal was preferred, because other calibration software like Calib or OxCal do not allow to calibrate radiocarbon ages back 50 ka BP. There was no need to apply any age correction, as a hard-water effect was neither detected for modern aquatic plants growing in the littoral zone of the lake nor for autochthonously precipitated carbonates (Haberzettl et al., 2005). For age-depth modeling the depth scale was event-corrected, i.e. the thicknesses of instantaneous events like volcanic ash layers and mass movement deposits were subtracted from the overall sediment thickness. This event-correction encompasses 60.29 m. The maximum chronostratigraphic sediment depth for age-depth modeling was thus reduced to 45.80 m cd-ec (m of event-corrected composite depth). For this corrected depth scale two age-depth models were developed using the mixed-effect regression after Heegaard et al. (2005): the first age-depth model by running two iterations with the mixed-effect regression and the second by running the mixed-effect regression only with ages that strictly follow the law of superposition. The mixed-effect regression is regarded as a method relatively robust with regard to outliers. In addition to the uncertainty of the individual radiocarbon date it considers how representative the dates are in relation to the population of other close by dates. This method also produces error margins for the established age-depth model. The statistical software Tinn-R (Version: 2.3.5.2) and the libraries mgcv and agedepth (downloaded from http://www.eecrg.uib.no/ on 3.11.2010) were used for calculations. To support the radiocarbon-based chronology, two additional stratigraphic methods were considered: tephrochronology and geomagnetic relative paleointensities.

To characterize volcanic ash layers, glass components of tephra samples were analyzed for their element geochemistry with an electron microprobe at the Tephrochronology Analytical Unit of the University of Edinburgh, UK. Analyses were performed on polished thin-sections on a five-spectrometer Cameca SX-100 electron microprobe with a beam diameter of 5 μm and an accelerating voltage (beam current) of 15 keV (2 nA) for major elements and 15 keV (80 nA) for minor elements. Standard calibration blocks and glass standards were used for calibration and control of accuracy during analyses.

The comparison of geomagnetic relative paleointensity focuses on the period from 55 to 25 cal. ka BP because this is the period most critical for chronology. The average initial temporal resolution in years (a) per individual data point of the records used are 11.34 a (age-model 1), 9.44 a (age-model 2), 10 a after cutoff frequency 1/3000 a (^{10}Be-flux to Summit in Greenland: Muscheler et al. (2005)), 48 a (SAPIS: Stoner et al. (2002)), 200 a (stack from the Mediterranean Sea and Somali Basin: Meynadier et al. (1992)) and 220 a (Lake Baikal: Peck et al. (1996)). The stack from the Mediterranean Sea and Somali Basin comprises the highest resolution records (>10 cm/ka) from the marine stack SINT-200 (Guyodo and Valet, 1996) and the stack from the South Atlantic Ocean (SAPIS: Stoner et al. (2002)) comprises five high-resolution records (14.9–25 cm/ka) located in the sub-Antarctic region. Each of the Laguna Potrok Aike datasets was interpolated at 10 a intervals, then smoothed in order to illustrate the millennial variability and, finally, the correlation coefficients were calculated. For more details on the paleomagnetic record of Laguna Potrok Aike, the reader is referred to Lisé-Pronovost et al. (in this issue).

4. Results

4.1. Lithology

The total length of the composite profile from Site 2 (5022-2CP) is 106.09 m and comprises 101.02 m of sediment (Fig. 2). Broken liners, ineffective core catchers and the lack of sedimentary features for core correlation caused 24 gaps summing up to the

Please cite this article in press as: Kliem, P., et al., Lithology, radiocarbon chronology and sedimentological interpretation of the lacustrine record from Laguna Potrok Aike, southern Patagonia, Quaternary Science Reviews (2012), http://dx.doi.org/10.1016/j.quascirev.2012.07.019

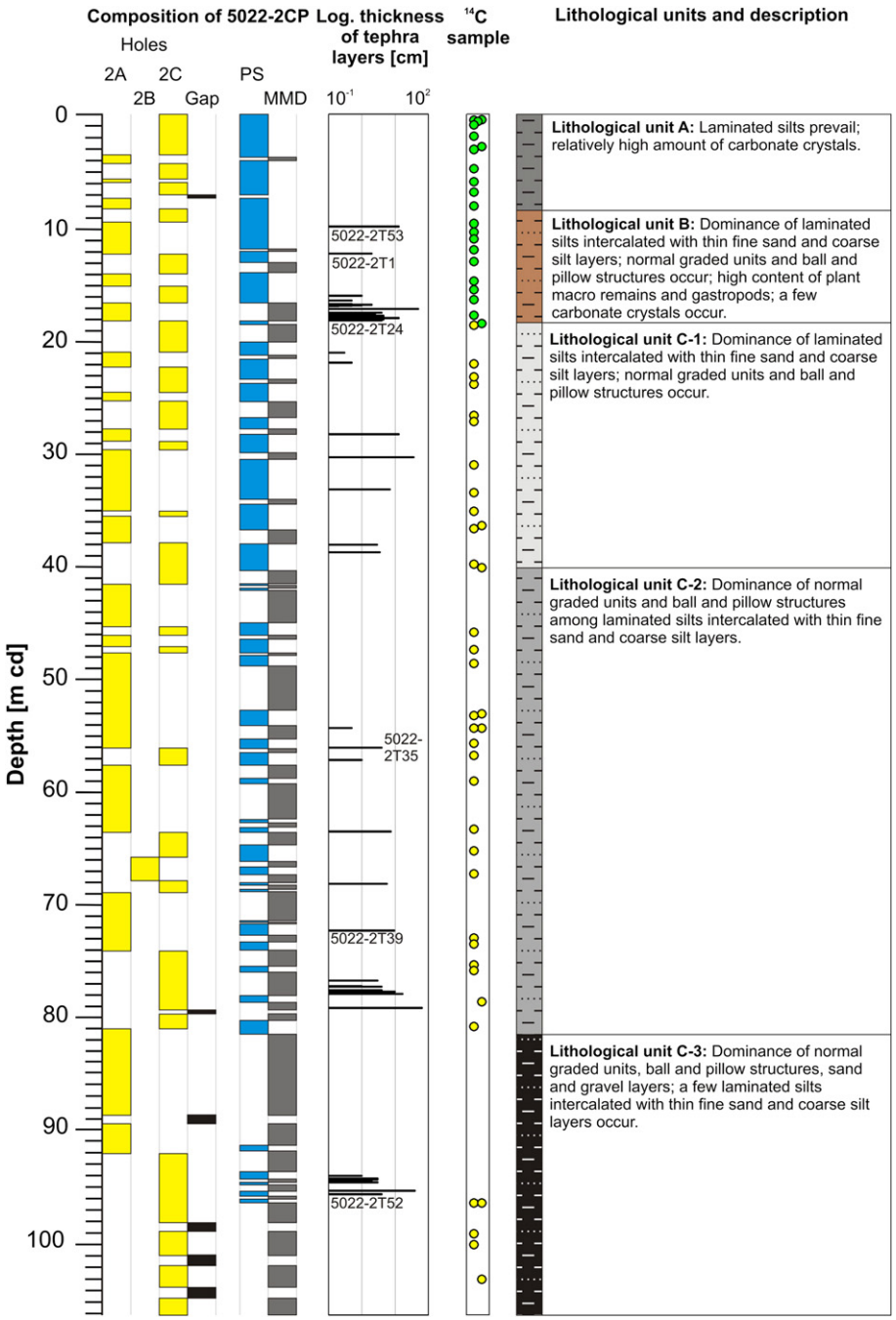

Fig. 2. Composition and lithology of the composite profile from site 2 (5022-2CP) of Laguna Potrok Aike. 2A, 2B and 2C: holes of site 2; PS: pelagic sediment; MMD: mass movement deposits and gaps illustrated if their thicknesses increase 10 cm. Tephra layers are indicated according to their average depths. Radiocarbon samples in green circles are correlated ages from PTA03/12 + 13 (Haberzettl et al., 2007); those in yellow are samples from 5022-2CP. (For interpretation of the references to color in this figure legend, the reader is referred to the web version of this article.)

missing 5.06 m. Six gaps of 52 cm thickness are assumed to theoretically have contained pelagic sediment as they are over- and underlain by this type of sediment. The remaining eighteen gaps of 454 cm in combined thickness are related to event deposits as they are either over- or underlain by very coarse-grained mass movement deposits. Often the very coarse-grained sediment from the basal units of mass movements caused broken liners or flushed-out sections and consequently created gaps in the record in 5022-2CP.

The composite profile consists of six different but recurring sediment structures: laminated silts (Fig. 3A), laminated silts intercalated with thin fine sand and coarse silt layers (Fig. 3B), ball and pillow structures (Fig. 3C), normally graded beds (Fig. 3D), structureless sand with fine gravel layers (Fig. 3E) and light-colored silt layers (Fig. 3H).

Laminated silts (Fig. 3A) have contributions of clay and small amounts of sand. The lamination is characterized by changing colors ranging from light to dark gray, greenish to bluish gray and brownish gray and is most distinct for the topmost 18 m. Laminae thickness varies in the cm- and dm-scale without any sharp boundaries. Laminated silts are interpreted as pelagic sediments as their accumulation results from continuous settling of particles through the water column to the lake floor.

Please cite this article in press as: Kliem, P., et al., Lithology, radiocarbon chronology and sedimentological interpretation of the lacustrine record from Laguna Potrok Aike, southern Patagonia, Quaternary Science Reviews (2012), http://dx.doi.org/10.1016/j.quascirev.2012.07.019

Laminated silts intercalated with thin fine sand and coarse silt layers (Fig. 3B) differ from laminated silts as they contain a few coarser layers which are millimeter-thick and dark gray to black in color. As these layers are homogenous or normally graded, the contact to the overlying sediment is either sharp or gradual while the contact to underlying laminated silts is always sharp. Laminated parts are interpreted as pelagic sediments, whereas the coarse-grained intercalations reflect event-deposits. The frequency of these event-deposits varies between one per centimeter to one per decimeter. Although their frequency can be high, their contribution to this sediment type remains low. Thus, they are not subtracted for event correction.

Normally graded beds interrupt pelagic sediments. In 5022-2CP they reach up to 3.5 m in thickness and mostly consist of three units: 1) a fining-upward base of dark gray to black coarse silt, sand or gravel often containing abundant plant fragments, 2) a homogeneous silt to clay layer and 3) a thin layer of light-colored clay and silt on top (Fig. 3D). Such structures in lacustrine sediments have been interpreted as turbidites or homogenites resulting from mass movements (Sturm et al., 1995; Girardclos et al., 2007; Bertrand et al., 2008).

Sometimes ball and pillow structures (Fig. 3C) underlie these graded beds and originate from the same mass movement. They consist of brownish, bluish or greenish-gray rounded silt and clay nodules up to several decimeters in size embedded in a dominantly coarse (up to gravel) and unsorted mostly dark gray matrix. Structureless sand and fine gravel layers (Fig. 3E) consist of homogenous, not graded blackish sands and/or fine gravel showing sharp upper and lower contacts. They reach a thickness of a few decimeters and sometimes contain organic macro remains (Fig. 6B). They are also interpreted as the result of mass movement deposits but very likely of a different type compared to normally graded beds.

Light-colored and sorted silt layers comprise bent, laminated or homogeneous sediment structures (Fig. 3H). Contacts to over- and underlying sediments are relatively sharp and sometimes irregular. Some layers show a coarser base of not more than 1 cm in thickness containing light-colored as well as black grains. Smear slides reveal a dominance of volcanic glass shards, pumice and amorphous clasts and sometimes also phenocrysts of volcanogenic minerals. Consequently, these deposits have been interpreted as tephra layers, which are distributed throughout 5022-2CP and reach individual thicknesses of up to 50 cm (Fig. 2). As all described tephra layers result from Andean volcanic eruptions in a distance of at least 150 km (Haberzettl et al., 2007, 2008), thick tephra layers probably not completely result from fallout, but also from lake internal reworking and fluvial or eolian reworking of volcanic ash material that was deposited in the sparsely vegetated steppe environment surrounding the lake. Some tephra layers actually show structures of reworking (bent layers, mixing with lacustrine sediment components). The coarser base of some tephras might be the effect of sorting after settling through the water column or the result of a gradual decrease in explosivity of the related volcanic eruption.

Based on the dominating sedimentary characteristics and on the degree of dominance of mass movement deposits, 5022-2CP is divided into five lithological units (Fig. 2):

Lithological unit A (0–8.82 m cd) is almost completely dominated by pelagic laminated silts. The color spectrum changes downwards from light and brownish gray to dark gray while lamination gets more diffuse. Smear slides show a relatively high content of carbonate crystals. Furthermore, low amounts of aquatic mosses and gastropods are characteristic for this unit.

Lithological unit B (8.82–18.72 m cd) mainly consists of pelagic laminated silts intercalated with thin fine sand and coarse silt layers. The color spectra of laminations vary between dark gray (in the upper part) and brownish and light gray (in the lower part). Furthermore, a few normally graded beds, ball and pillow structures as well as homogenous sand layers occur. The thickness of normally graded beds does not exceed 20 cm while clay caps are absent. Their color spectrum varies from brownish gray at the top to

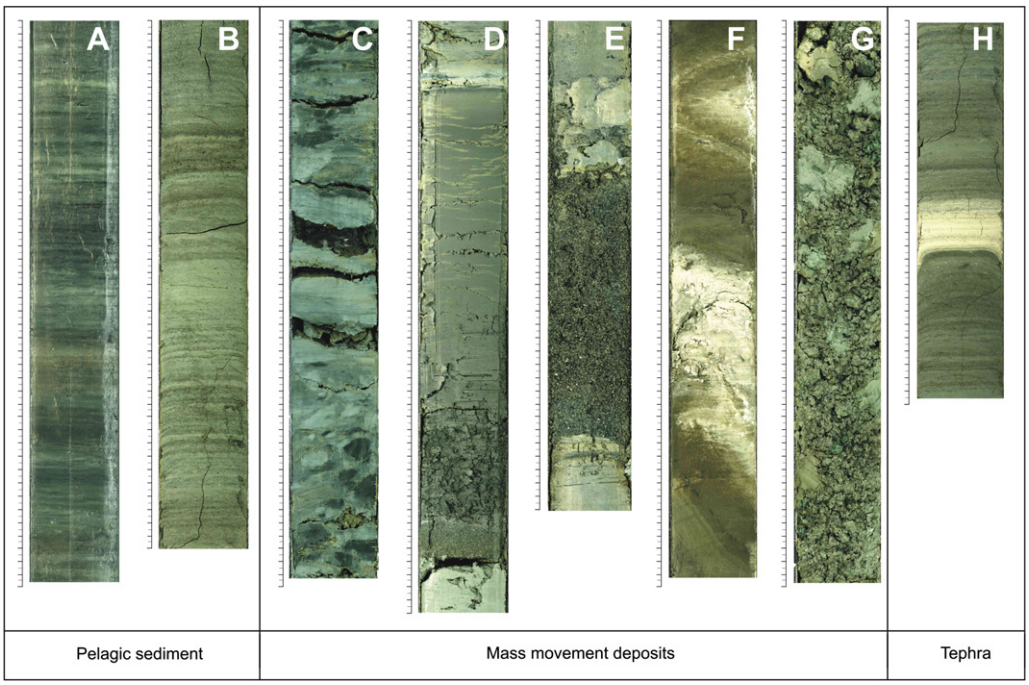

Fig. 3. Different classes of sediment structures from 5022-2CP. The scale to the left of each photography is in cm. A) Laminated silts (1.87–2.28 m cd), B) Laminated silts intercalated with thin fine sand and coarse silt layers (55.49–55.90 m cd), C) ball and pillow structure (19.45–19.88 m cd), D) Normally graded beds (21.38–21.93 m cd), E) Structureless sand and fine gravel layer (34.18–34.56 m cd), F) unique folded layer (77.45–77.99 m cd), G) unique matrix supported structure (87.92–88.36 m cd), H) Light-colored layer of sorted silt (55.80–56.08 m cd). (For interpretation of the references to color in this figure legend, the reader is referred to the web version of this article.)

Please cite this article in press as: Kliem, P., et al., Lithology, radiocarbon chronology and sedimentological interpretation of the lacustrine record from Laguna Potrok Aike, southern Patagonia, Quaternary Science Reviews (2012), http://dx.doi.org/10.1016/j.quascirev.2012.07.019

dark gray at the base. These sediment structures deviate from the thicker and clay-capped graded units which dominate the underlying lithological unit C. A high amount of aquatic mosses occurs between 15 and 18.6 m cd. Gastropods are relatively frequent as well as a few fish bones and carbonate crystals above 14.2 m cd.

Lithological unit C (18.72–106.09 m cd) is subdivided into three subunits (C-1, C-2, C-3) according to percentage, frequency and thickness of mass movement deposits. No gastropods, bones or carbonate crystals occur in this unit.

Lithological unit C-1 (18.72–40.23 m cd) is dominated by pelagic laminated silts intercalated with thin fine sand and coarse silt layers. The lamination is poor in contrast to lithological units A and B. The color spectrum turns to greenish and bluish gray. All three identified types of mass movement deposits (normally graded beds; ball and pillow structures; structureless sand and fine gravel layers) occur.

Lithological unit C-2 (40.23–81.53 m cd) is mainly composed of the same sedimentary structures as lithological unit C-1. However, the percentage of mass movement deposits increases (Fig. 2) and some events exceed 1 m in thickness. The majority of mass movement deposits consists of normally graded beds, some of them containing fine gravel at the base. A prominent feature is one folded structure of pelagic sediment and tephra (Fig. 3F) followed by a 90 cm thick normally graded bed.

Lithological unit C-3 (81.53–106.09 m cd) is dominated by normally graded sediment structures which typically increase 1 m in thickness. Pelagic sediments are almost absent and the amount of gravel in mass movement deposits is generally higher compared to units C-1 or C-2. Fine gravels occur in some ball and pillow structures as well as at the base of normally graded beds. One outstanding and 1.5 m thick matrix supported layer occurs at 88 m cd. It consists of angular silt and clay clasts in a matrix of basaltic sand and gravel (Fig. 3G). The clasts appear to be remobilized pelagic sediments as lamination is preserved in some of these clasts and the angular morphology suggests a short-distance transport. The angular basaltic gravel probably originates from erosion of basaltic lava at the southwestern lake shore.

4.2. Tephra analyses and correlation

Prior to this study, six tephra layers have been documented in different sediment cores from Laguna Potrok Aike (Haberzettl et al., 2009). The upper three ash layers from PTA03/12 + 13 were correlated stratigraphically to 5022-2CP (Fig. 5), while the older three tephra layers were geochemically compared with microprobe data obtained from a total of 19 volcanic ashes from 5022-2CP (Wastegård et al., in this issue).

The latest compilation of available dates for the upper three tephra layers from the Andean volcanoes Hudson, Mt. Burney and Reclús was published by Stern (2008) and recalibrated with the CalPal_2007_HULU calibration curve (Table 3). In the case of the Mt. Burney ash layer, three geochemically indifferent Mt. Burney eruptions have been documented between the Hudson and Reclús tephras spanning the time window from 7,64 to 10,320 cal. BP (Kilian et al., 2003). For the sediments of Laguna Potrok Aike, only one Mt. Burney tephra occurs between Hudson and Reclús ash layers. This volcanic ash has been correlated to the youngest Mt. Burney tephra layer (Haberzettl et al., 2007), which is interpreted as the major eruption with a large ash fan whereas the other two eruptions produced only local ash deposits (Kilian et al., 2003).

The lower three ash layers from Mt. Burney and Reclús volcanoes described by Haberzettl et al. (2007, 2008, 2009) are geochemically identical with 5022-2T35, 5022-2T39 and 5022-2T52 (Table 1) and have been used for correlation. Analyses show that 5022-2T39 and 5022-2T52 are rhyolitic with SiO_2 values ranging from 74 to 77% and K_2O values from 1.5 to 1.7% (Fig. 4A) suggesting Mt. Burney as the volcanic source (Stern, 2008; Haberzettl et al., 2009). Although the geochemical composition is similar, 5022-2T39 has a higher contents in MgO, FeO_{tot} and CaO compared to 5022-2T52 (Fig. 4B) and can be clearly distinguished. The main component of 5022-2T35 (type a) has a dacitic composition making it difficult to determine the source of the volcanic eruption. The SiO_2 vs. K_2O scatterplot (Fig. 4) indicates volcanoes of

Table 1
Geochemical data of tephra layers 5022-2T35, 5022-2T39 and 5022-2T52, shown as mean oxide concentrations (wt %) and 1 standard deviation in parentheses. Only analyses above 94% are included in the means (*n*: number of analyses).

	5022-2T35 (type a)	5022-2T35 (type b)	5022-2T39	5022-2T52
n	9	2	24	14
SiO_2	68.70 (1.34)	73.76 (0.26)	71.64 (0.75)	73.57 (0.93)
TiO_2	0.52 (0.05)	0.12 (0.02)	0.35 (0.02)	0.25 (0.02)
Al_2O_3	14.74 (0.29)	12.38 (0.86)	12.93 (0.27)	12.63 (0.23)
FeO_{tot}	2.73 (0.13)	1.23 (0.30)	1.92 (0.10)	1.42 (0.10)
MnO	0.05 (0.01)	0.04 (0.03)	0.05 (0.01)	0.04 (0.01)
MgO	0.84 (0.15)	0.29 (0.13)	0.52 (0.03)	0.38 (0.03)
CaO	3.07 (0.12)	1.38 (0.06)	2.31 (0.10)	1.84 (0.14)
Na_2O	4.23 (0.13)	3.58 (0.37)	4.51 (0.13)	4.55 (0.17)
K_2O	2.38 (0.06)	3.22 (0.14)	1.60 (0.07)	1.60 (0.07)
P_2O_5	0.10 (0.01)	0.03 (0.01)	0.05 (0.01)	0.04 (0.01)
Total	**97.36 (1.83)**	**96.03 (1.37)**	**95.88 (0.94)**	**96.33 (1.15)**

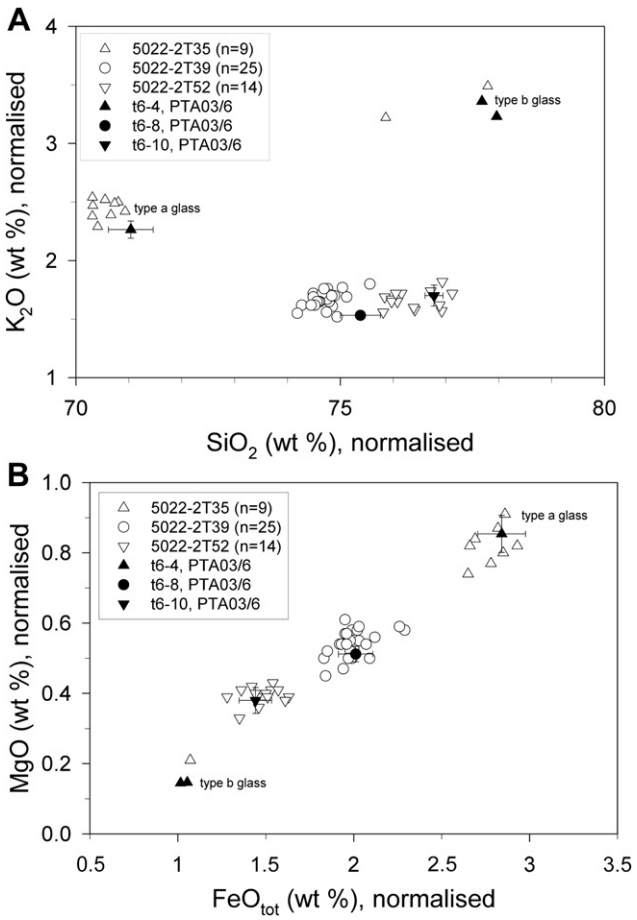

Fig. 4. Microprobe analyses of selected tephra layers from Laguna Potrok Aike (for all analyzed data: see Wastegård et al., in this issue). All data from PTA03/6 show mean values and 1 sd (standard error) (Haberzettl et al., 2008 and Wulf, personal communication, 2010). A) Bi-plot of SiO_2 vs. K_2O, B) Bi-plot of FeO_{tot} vs. MgO. All data are normalized to 100%.

the Northern Andean Volcanic Zone (NAVZ) as a potential source, i.e. volcanoes Viedma, Lautaro or Aguilera (Kilian et al., 2003; Stern, 2008). In contrast, a tephra layer with a similar geochemistry was inferred to be an older Reclús tephra by Haberzettl et al. (2008). A minor rhyolitic component (type b) was also analyzed for this tephra.

All three geochemically analyzed tephras can be correlated with tephras from core PTA03/6 (Haberzettl et al., 2008) (Fig. 4). The rhyolitic ashes are correlated with tephra layers at 643 cm (t6–8) and 859 cm (t6–10) of PTA03/6 while both glass components of 5022-2T35 correspond to tephra layer t6–4 at 359 cm of PTA03/6. The agreement between the different analyses is high and the small deviations in glass chemistry (e.g. slightly higher SiO_2 values in Haberzettl et al. (2008)) are probably due to different instruments and analytical procedures applied.

4.3. Radiocarbon dates, chronology and sedimentation rate

For the Holocene and the Lateglacial part of the lacustrine record from Laguna Potrok Aike radiocarbon dating was carried out on carbonates precipitated from the water column, bulk sediment and different organic macro remains (Haberzettl et al., 2007). As carbonates are generally absent below 18 m cd for 5022-2CP, plant remains, in most cases stems of aquatic mosses, were the only biogenic sediment component available for AMS ^{14}C dating. These aquatic mosses are concentrated in layers intercalated within pelagic sediment sections (Fig. 6A) as well as in basal layers of mass movement deposits (Fig. 6B). The former were preferably sampled because the likelihood of obtaining ages that do not represent the time of deposition is much higher for mass movement deposits. Nevertheless, dating was also carried out for some samples from such deposits in order to obtain ^{14}C ages over the entire length of the composite sediment sequence. In general, dating of aquatic mosses might involve some degree of reworking at Laguna Potrok Aike. An alternative option would be to obtain other material for dating (e.g. pollen, aquatic algae) which is not concentrated in layers. This would not necessarily eliminate reservoir effects and was not performed at 5022-2CP as it implies to sieve large amounts of pelagic sediment.

In total, 58 radiocarbon dates are available (Table 2; Fig. 7). 21 ages were correlated from PTA03/12 + 13 for the upper 18 m of 5022-2CP. These comprise the last 16 cal. ka BP. Three dates were interpreted as reworked (Haberzettl et al., 2007) and thus omitted.

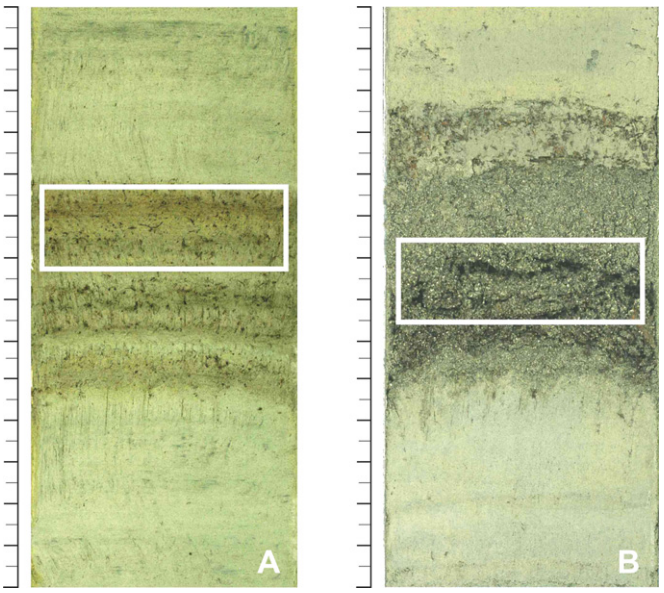

Fig. 6. Layers with high concentration of plant macro remains from aquatic mosses in A) Laminated silts (related radiocarbon date: POZ-32495) and B) In a structureless sand layer (POZ-32492). Both positions were used for radiocarbon dating; white boxes show sampling location.

In order to achieve a consistent interpretation, Poz-8391 and Poz-5071 were reinterpreted as event deposit as the former was obtained from a sand-layer and the latter from reworked Reclús tephra of PTA03/12 + 13. Below 18 m cd, 37 dates cover a time range between 18 and 51 cal. ka BP. Extremely low ^{14}C values were measured for three samples yielding infinite ages (Table 2). These ages were excluded from age-depth modeling.

Intervals with mass movement deposits as well as tephra layers were removed to compile an event-corrected composite profile (cd-ec) for age-depth modeling which was carried out by mixed-effect regression for 45.80 m cd-ec. This method is regarded to be relatively robust to outliers (Heegaard et al., 2005). However, it ignores the law of superposition. Two age-models (1 and 2) have been developed, one following the mixed-effect regression and the other by additionally acknowledging the law of superposition.

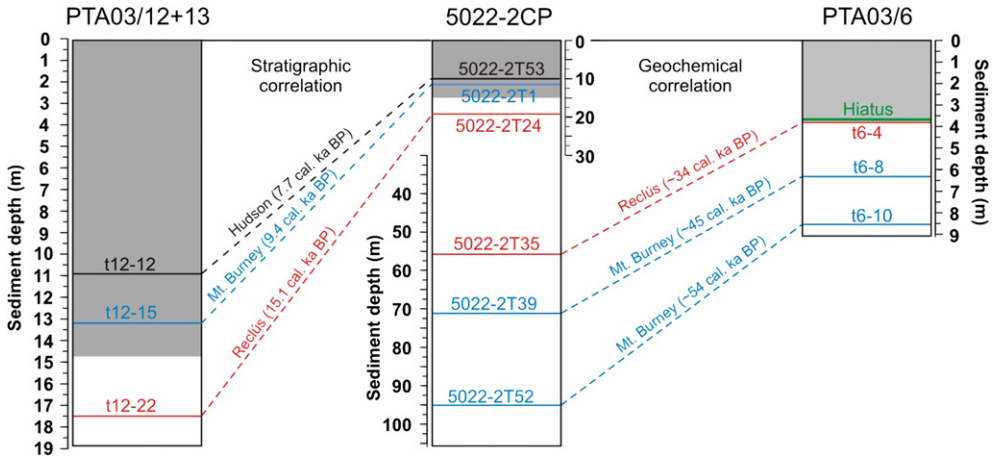

Fig. 5. Stratigraphic tephra correlation of 5022-2CP (100 m water depth) with PTA03/12 + 13 (95 m water depth) and geochemical tephra correlation of 5022-2CP with PTA03/6 (30 m water depth). Ages of tephra layers t12–12, t12–15 and t12–22 are recalibrated after Stern (2008) and t6–4, t6–8 and t6–10 are from Haberzettl et al. (2009). The hiatus of PTA03/6 was caused by erosion due to a low lake level (Haberzettl et al., 2008; Anselmetti et al., 2009). Note different depth scales. Gray shading marks Holocene deposits.

Please cite this article in press as: Kliem, P., et al., Lithology, radiocarbon chronology and sedimentological interpretation of the lacustrine record from Laguna Potrok Aike, southern Patagonia, Quaternary Science Reviews (2012), http://dx.doi.org/10.1016/j.quascirev.2012.07.019

Table 2
AMS radiocarbon ages from 5022-2CP of Laguna Potrok Aike calibrated with CalPal applying the CalPal_2007_HULU calibration curve. Ages from reworked sediment sections are printed in bold. $\delta^{13}C$ and C-mass as measured during AMS ^{14}C determination.

Laboratory no.	Sediment depth (m cd)	Event corrected sediment depth (m cd-ec)	^{14}C age (BP)	Error (1σ)	$\delta^{13}C$ (‰)	C-mass (mg)	Sample description	Calibrated age (cal. BP)	Error (1σ)
Poz-834[a]	0.51	0.51	440	30	−22.7	0.85	Stems of aquatic moss	510	30
Poz-897[a]	0.56	0.55	655	25	−15.7	1.49	Bulk sediment	630	50
Poz-3570[a]	0.67	0.67	735	25	−8	1.30	Calcite fraction of bulk sample	690	20
Poz-896[a]	0.92–1.04	0.92–1.04	1470	40	−20.8	2.0	Stems of aquatic moss	1370	40
Poz-5182[b]	1.96	1.95	2300	35	−22.7	1.57	Twig of Berberis	2290	70
Poz-8549[b]	2.88	2.87	3600	35	2.2	6.28	Calcite fraction of bulk sample	3910	50
Poz-8390[b]	3.10–3.15	3.10–3.15	3625	35	−33.9	0.5	Stems of aquatic moss	3940	50
Poz-8398[b]	4.83	4.53	4465	50	−28.3	1.09	Stems of aquatic moss	5130	120
Poz-8550[b]	6.00	5.71	6440	70	−5.1	6.28	Calcite fraction of bulk sample	7360	60
Poz-8391[b]	6.91	6.63	7025	50	−21.5	0.51	**Stems of aquatic moss**	7870	60
Poz-8546[b]	8.12	7.83	7260	50	3.8	2.01	Calcite fraction of bulk sample	8090	60
Poz-8392[b]	9.69	9.37	7580	50	−28.3	2.56	Stems of aquatic moss	8390	40
Poz-8393[b]	10.44	9.97	9640	50	−28.4	2.43	**Stems of aquatic moss**	11,000	140
Poz-8547[b]	11.00–11.08	10.53–10.61	9410	50	6.6		**Calcite fraction of bulk sample**	10,640	60
Poz-8394[b]	12.00	11.37	11,090	60	−26.8	1.94	**Stems of aquatic moss**	12,980	80
Poz-5985[b]	13.04	12.22	8930	50	−18.9	2.28	Bone of Tuco Tuco	10,060	110
Poz-8548[b]	14.78	13.00	10,240	60	8.4	3.61	Calcite fraction of bulk sample	11,970	130
Poz-8396[b]	15.55	13.78	11,200	60	−30	1.69	Stems of aquatic moss	13,130	80
Poz-8397[b]	16.40	14.61	12,490	70	−31.2	1.60	Stems of aquatic moss	14,900	140
Poz-5072[b]	16.78–18.20	14.70	12,850	70	−25.8	2.64	**Stems of aquatic moss**	15,420	90
Poz-5073[b]	18.48–18.54	14.93–14.99	13,450	70	−28.7	2.69	Stems of aquatic moss	16,710	100
Poz-37017	18.69	15.13	14,540	70	−27.6	1.56	Stems of aquatic moss	17,760	50
Poz-37022	22.09	16.74	17,460	80	−29.2	1.63	Stems of aquatic moss	20,970	120
Poz-37007	23.25	17.90	18,700	120	−39.9	0.91	Stems of aquatic moss	22,570	110
Poz-32491	23.90	18.23	27,910	240	−25.9	2.12	**Stems of aquatic moss**	32,420	280
Poz-34233	26.65	19.42	22,450	140	−30.7	2.24	**Stems of aquatic moss**	27,230	320
Poz-37020	27.20	19.69	20,490	120	−28	1.11	Stems of aquatic moss	24,510	150
Poz-37008	31.01	22.14	30,300	300	−32.9	1.51	Stems of aquatic moss	34,500	240
Poz-37010	33.45	24.46	47,000	2000	−23.5	1.40	Organic macro remains	50,590	2670
Poz-34235	35.10	25.49	26,930	210	−28.5	3.03	**Stems of aquatic moss**	31,720	140
Poz-34236	36.38	26.67	25,110	180	−25	1.45	Stems of aquatic moss	30,030	170
Poz-34237	36.66	26.95	25,820	190	−27.3	2.64	Stems of aquatic moss	30,750	320
Poz-32492	39.77	28.69	34,500	500	−27.7	2.54	**Stems of aquatic moss**, Fig. 6B	39,770	910
Poz-37011	40.09	28.98	29,300	300	−28.9	1.86	Stems of aquatic moss	33,700	350
Poz-37012	45.81	30.30	31,900	300	−28.3	2.33	Organic macro remains	35,780	380
Poz-37002	47.34	31.34	29,600	300	−30.7	1.24	Stems of aquatic moss	33,930	310
Poz-37013	48.58	32.32	40,000	1000	−28	2.27	Stems of aquatic moss	43,730	810
Poz-34238	52.98	32.82	37,300	800	−28.5	2.37	Stems of aquatic moss	42,040	500
Poz-37003	53.12	32.96	39,200	700	−28.6	1.64	Stems of aquatic moss	43,140	570
Poz-32493	54.23	33.88	27,680	230	−24.3	1.30	**Stems of aquatic moss**	32,230	230
Poz-37014	54.23	33.88	44,000	2000	−24	1.18	**Stems of aquatic moss**	47,450	2200
Poz-37075	55.59	34.15	30,800	400	−18.1	0.63	Stems of aquatic moss	34,920	380
Poz-34239	56.66	34.71	42,000	2000	−28.7	2.25	Stems of aquatic moss	45,610	1850
Poz-34240	58.91	36.00	43,000	2000	−30	1.29	Stems of aquatic moss	46,510	2040
Poz-34241	63.18	36.70	50,000	3000	−30.4	2.36	Stems of aquatic moss	53,610	3630
Poz-37018	65.11	37.33	43,000	2000	−26.8	2.13	Organic macro remains	46,510	2040
Poz-32494	67.13	38.87	43,000	2000	−28.3	1.08	Stems of aquatic moss	46,510	2040
Poz-34242	72.80	40.56	44,000	2000	−30.3	2.43	Stems of aquatic moss	47,450	2200
Poz-37004	73.32	40.66	47,000	2000	−39.7	1.71	Stems of aquatic moss	50,590	2670
Poz-34243	75.18	41.40	47,000	2000	−34.8	2.27	**Stems of aquatic moss**	50,590	2670
Poz-37006	75.68	41.67	51,000	4000	−32.3	1.50	Stems of aquatic moss	53,910	4130
Poz-37021	78.43	42.39	>48,000		−18.9	1.18	Organic macro remains		
Poz-32495	80.60	42.97	45,000	2000	−27.2	1.64	Stems of aquatic moss, Fig. 6A	48,430	2320
Poz-34245	96.21	45.71	>48,000		−30.4	2.46	Stems of aquatic moss		
Poz-37015	96.21	45.71	52,000	4000	−27.2	1.26	Organic macro remains	54,580	3940
Poz-37016	98.95	45.79	42,000	1000	−26.2	1.06	Organic macro remains	45,200	1060
Poz-34246	99.89	45.80	50,000	4000	−30.6	2.05	**Stems of aquatic moss**	53,220	4250
Poz-32496	102.96	45.80	>45,000		−32	0.82	**Stems of aquatic moss**		

[a] Haberzettl et al. (2005).
[b] Haberzettl et al. (2007).

For age-model 1 (Fig. 8A and B) thirteen dates on remobilized material were excluded prior to the mixed-effect regression. The first iteration (Fig. 8A) reveals that (1) some radiocarbon dates considerably exceed the 95% confidence interval of the calculated age-depth model and (2) the age-depth modeling below 43 m cd-ec produces an age reversal caused either by a lack of reliable material for dating or because the radiocarbon method is close to its age-limit (>45 cal. ka BP). Therefore, a second iteration with the mixed-effect regression was restricted to dates above 43 m cd-ec (two more dates were not considered) and excludes four dates considerably exceeding the confidence interval of the first iteration (Fig. 8B). As this chronology does not extent to the base of the composite record, the age-depth model was extrapolated below 43 m cd-ec down to a basal depth of 45.80 m cd-ec resulting in an age of 51.2 cal. ka BP. This is the maximum age for 5022-2CP with age-model 1 as only event deposits occur below.

Please cite this article in press as: Kliem, P., et al., Lithology, radiocarbon chronology and sedimentological interpretation of the lacustrine record from Laguna Potrok Aike, southern Patagonia, Quaternary Science Reviews (2012), http://dx.doi.org/10.1016/j.quascirev.2012.07.019

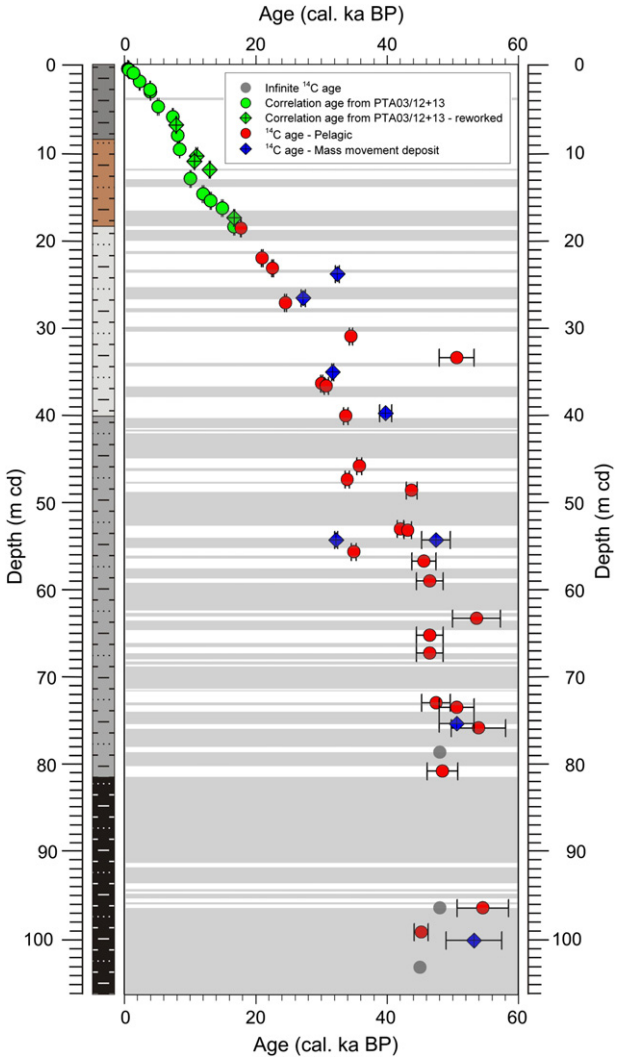

Fig. 7. Depth distribution of ^{14}C ages in 5022-2CP (1σ error). Lithology and event deposits (gray shading) are indicated.

Age-model 2 was developed on the youngest possible radiocarbon ages and strictly according to the law of superposition (Fig. 9). Thus not only radiocarbon ages on some of the reworked material (iteration 1) and dates excluded during iteration 2 were discarded but a total number of 29 calibrated dates (19 for age-model 1). Hence, age-model 2 is based only on four dates below 20 m cd-ec. Most of the discarded radiocarbon ages exceed the 95% confidence interval of age-model 2. The extrapolation below 44.79 m cd-ec yields a bottom age of 45.2 cal. ka BP for the basal depth of 45.80 m cd-ec.

In order to validate these age-depth models, we compared the PTA03/12 + 13 age-depth relation with age-models 1 and 2 for the last 16 cal. ka BP based on their magnetic susceptibility records (Fig. 10). Generally, they show a fairly good correlation with PTA03/12 + 13 suggesting a consistent age transfer to 5022-2CP. Slight shifts of magnetic susceptibility peaks between 8 and 10 cal. ka BP and prior to 12 cal. ka BP result from differences of our age model compared to the model performed by Haberzettl et al. (2007). They used a linear interpolation and included the Mt. Burney tephra (t12–15) dated by Kilian et al. (2003) for their age model. The upper three tephras from PTA03/12 + 13 have been dated independently by peat bogs and lake sediments (Kilian et al., 2003; McCulloch et al., 2005; Stern, 2008) and tend to be younger than the estimated ages from both of our age models; but their 95% confidence intervals overlap (Table 3).

The tephra correlation beyond 30 cal. ka BP from PTA03/6 to 5022-2T35 seems to confirm age-model 2, whereas the correlation to 5022-2T39 and to 5022-2T52 seems to verify age-model 1 (Figs. 8 and 9). However, the age of 5022-2T35 as obtained from PTA03/6 is not very reliable because it results from a linear interpolation between a ^{14}C dated tephra layers ca 5 m above (14.9 ± 0.3 cal. ka BP) and at 3.5 m below (48.5 ± 2.5 cal. ka BP) this tephra. Moreover, it is a combination of two different coring locations from the slope of the lake basin (Haberzettl et al., 2009). Here we improve the dating of these tephra layers by applying age-model 1 (Table 3).

Finally, relative paleointensity results (cf. Lisé-Pronovost et al., in this issue) were compared with independently dated records worldwide to further validate our age models (Fig. 11). The millennial-scale variability using age-model 1 correlates much better to the global dipole field derived from independent archives, including cosmogenic isotopes, marine and lacustrine sediments (Meynadier et al., 1992; Guyodo and Valet, 1996; Peck et al., 1996; Stoner et al., 2002; Muscheler et al., 2005). In all cases, the correlation coefficients are significantly higher using age-model 1 compared to age-model 2 (Fig. 11). The minimum in relative paleointensity at ca 38–39 cal. ka BP (using age-model 1), coeval with the intensity low derived from the ^{10}Be flux of the Summit ice core from Greenland, might correspond to the Laschamp geomagnetic excursion (Lisé-Pronovost et al., in this issue), which was dated to 40.4 ± 2 ka (2σ) on lava flows at the type locality in the Massif Central, France (Guillou et al., 2004). Some of the differences in the paleointensity records most likely result from temporal offsets associated with the individual chronologies, which are to the limits of the radiocarbon method at 35–50 cal. ka BP (Hughen, 2007). This is illustrated, for example, by comparing SAPIS and PASADO records, where the correlation coefficient would be higher if the chronologies were slightly adjusted within dating uncertainties. Nonetheless and even on their own chronologies, the good correspondence between the SAPIS and PASADO records between 40 and 50 cal. ka BP supports age-model 1.

In conclusion, age-model 1 is favored and was used to calculate sedimentation rates for event-corrected 5022-2CP (Fig. 8C). Three periods are noticeable during which sedimentation rates exceed 1 mm/a: 6.6–9.4 ka BP, 23.7–31.1 ka BP and 46.3–51.2 ka BP. Minima occur at ~3 cal. ka BP (0.75 mm/a), ~15 cal. ka BP (0.37 mm/a) and ~38 cal. ka BP (0.40 mm/a). The event-corrected sedimentation rate averages 0.9 mm/a. Including the mass movement deposits it increases to 2.07 mm/a.

5. Discussion

5.1. Lithology

The lithological units coincide with the mid to late Holocene (lithological unit A: present to 8.3 cal. ka BP) and the Glacial period (lithological unit C: 17.2–51.2 cal. ka BP) separated by a transitional zone that started prior to the Lateglacial and ended in the early Holocene (lithological unit B: 8.3–17.2 cal. ka BP) (Fig. 8B). This transition is well defined in the lower part of lithological unit B by the highest concentration of plant macro remains within the entire record. The abrupt onset of plant macro remains at 17.2 ± 0.5 cal. ka BP suggests a climatic and a related environmental change that persists until 12.2 ± 0.7 cal. ka BP. This corresponds with the time range between the first (~19–17 cal. ka BP) and the second (~13–12 cal. ka BP) major deglacial warming steps documented from marine sediments off Chile and Antarctic ice records (Lamy et al., 2007). This is also confirmed by the continental record

Please cite this article in press as: Kliem, P., et al., Lithology, radiocarbon chronology and sedimentological interpretation of the lacustrine record from Laguna Potrok Aike, southern Patagonia, Quaternary Science Reviews (2012), http://dx.doi.org/10.1016/j.quascirev.2012.07.019

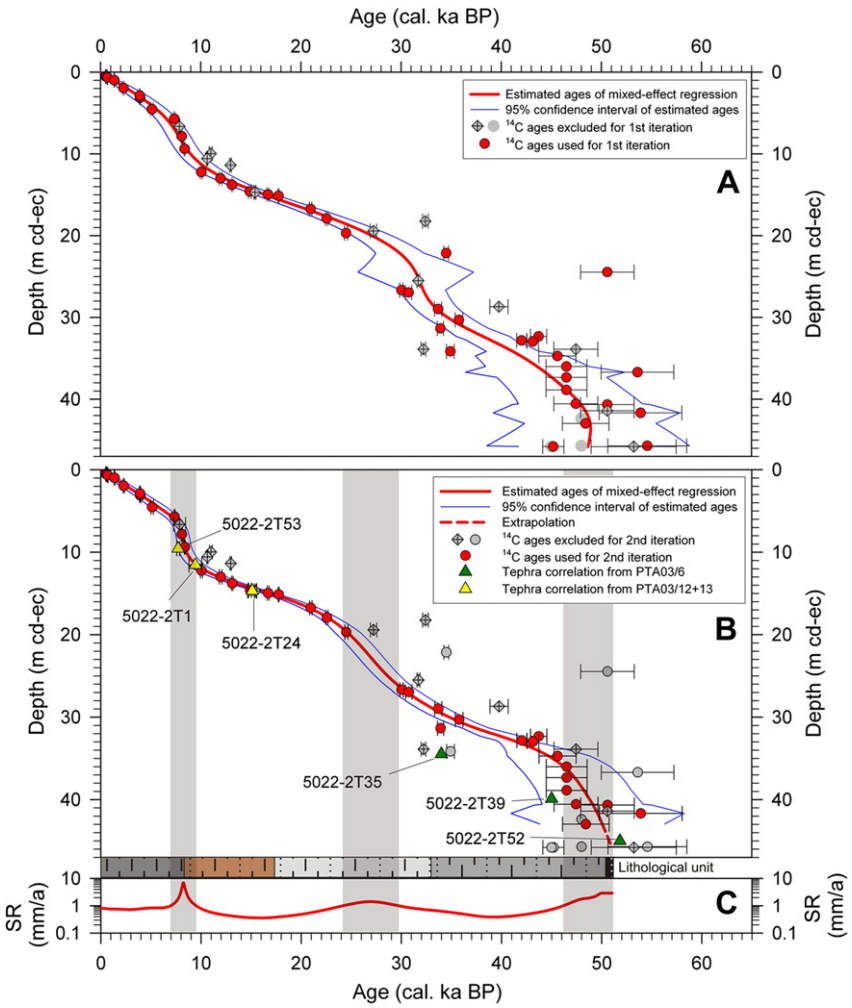

Fig. 8. First (A) and second (B) iteration (age-model 1) of the mixed-effect regression for 5022-2CP-ec using the constant–variance function. (C) Sedimentation rate based on this age-depth model processed for each millimeter. Gray shading marks periods with increased sedimentation rates. Tephra correlation according to Haberzettl et al. (2008, 2009).

from Lago Pollux (Chile, 46°S) suggesting deglacial warming after 18.6 cal. ka BP (Markgraf et al., 2007). Moreover, based on exposure ages deglaciation started in Patagonia after a final glacier advance at around 18 ka (Hein et al., 2010).

The high amount of plant macro remains (aquatic mosses) might result from an increased productivity due to deglacial warming and increased nutrient availability. As sand-wedges document former permafrost in southern Patagonia (Bockheim et al., 2009), its decay might have released organic carbon and nutrients in the drainage basin (Frey and Smith, 2005) which increased lacustrine productivity, predominantly in the littoral zone which is where aquatic mosses grow. However, it has been shown that recent permafrost degradation in the subarctic did not directly affect the trophic state of a lake and thus its sediments (Kokfelt et al., 2009).

Increased productivity of the lake is one possibility to explain the abundance of plant macrofossils at the transition from the Last Glacial Maximum (LGM) to the Lateglacial. Another explanation could be related to lake level fluctuations. Based on luminescence dates from overflow terraces, the lake level was highest around 17 cal. ka BP (Kliem et al., in this issue). Thus the transition from lithological unit C-1 to B might be a sedimentary response to the start of a post-LGM lake level lowering. This might have continued until 13.6 cal. ka BP, when the threshold of the lacustrine system with regard to carbonate precipitation was passed (Hahn et al., in this issue; Jouve et al., in this issue). Thus it might be argued, that the lake level during the early Lateglacial was comparable to modern conditions. A lake level decrease could also explain why aquatic mosses are so common immediately after 17 cal. ka BP: they were eroded from the freshly exposed former littoral zone of the lake. However, this would have caused additional profundal accumulation. In contrast, the period is characterized by very low sedimentation rates (Fig. 8).

Laminations of lithological units A and B range in thickness from cm- to dm-scales with sedimentation rates from 0.37 to 1 mm/a. They seem to reflect changes in depositional conditions of decadal to centennial timescales. The processes generating these laminations are not clear but must have been more pronounced during the Holocene and the Lateglacial with rather distinct laminations. This is also supported by smear slide analyses. Assuming that the occurrence of autochthonous carbonate crystals indicates warmer and drier climatic conditions with responding lower lake levels for the Holocene and the Lateglacial (Haberzettl et al., 2007), no such period with carbonate precipitation occurred during the recovered glacial record at Laguna Potrok Aike.

Intercalations of thin fine sand and coarse silt layers in laminated silts as well as mass movement deposits increase below lithological unit A. Thus, the lacustrine sedimentation pattern was completely different between the Holocene and the glacial period with the Lateglacial as a transition. Nevertheless,

Please cite this article in press as: Kliem, P., et al., Lithology, radiocarbon chronology and sedimentological interpretation of the lacustrine record from Laguna Potrok Aike, southern Patagonia, Quaternary Science Reviews (2012), http://dx.doi.org/10.1016/j.quascirev.2012.07.019

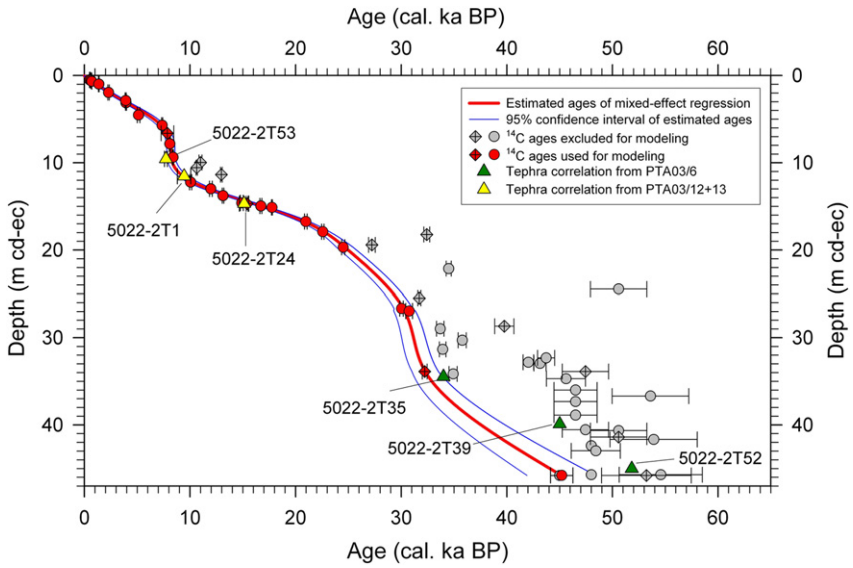

Fig. 9. Mixed-effect regression for 5022-2CP-ec using the constant–variance function. Ages for modeling were selected strictly according to the law of superposition (age-model 2).

also Holocene mass movement deposits have been identified by seismic and sediment core data (Haberzettl et al., 2007, 2008; Anselmetti et al., 2009). Earthquakes as well as very low lake levels during the early Holocene might have triggered these events. In the case of multiple and simultaneous mass movements in the entire lake basin, as identified by seismic analysis, earthquakes were likely the trigger (Anselmetti et al., 2009). In addition, very low lake levels can decrease slope stability because of increased sedimentation on tilted subaquatic strata (Hampton et al., 1996; Locat and Lee, 2002; Strasser et al., 2007) and in combination with pore-fluid overpressure (Sultan et al., 2004). The latter might be the effect of a reduced water column in combination with increased deposition of fine-grained sediments on subaqueous slopes potentially closing off pore water under undrained conditions (Anselmetti et al., 2009). The relative position between mass movement deposits and erosional gaps suggests a successive collapse of subaquatic terraces (Kliem et al., in this issue).

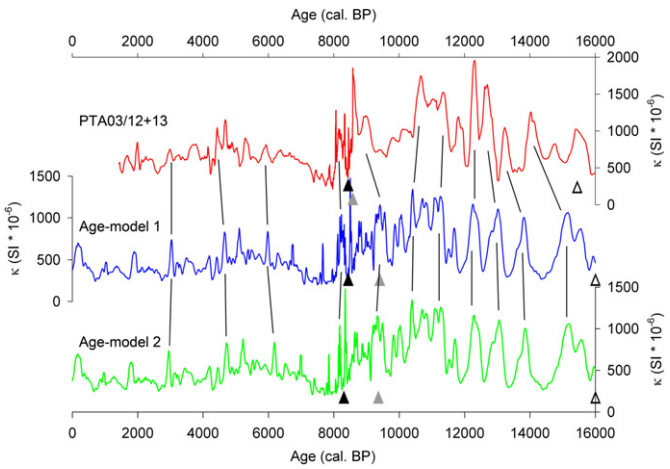

Fig. 10. Correlation of magnetic susceptibility from PTA03/12 + 13 and 5022-2CP with age-model 1 and age-model 2 using 11-point running means. Ages of PTA03/12 + 13 have been recalibrated with the CalPal_2007_HULU calibration curve prior to linear interpolation according to Haberzettl et al. (2007). Triangles show tephra layers with their ages in the respective age model.

As high-resolution data of the 3.5 kHz seismic survey allows sediment penetration only down to ~20 m (Anselmetti et al., 2009), no identification of simultaneous mass-movement events and thus paleo-earthquakes is possible below. It is likely that repeated lake level fluctuations during the last glacial period as well as earthquakes have resulted in frequent slope collapses which have not yet been detected. However, the maximum in mass movement frequency during the last glacial period is most likely the effect of environmental changes and not a paleo-earthquake signal. Probably, permafrost in combination with sea-level-controlled groundwater influence enforced lake level fluctuations. Frozen ground reduces infiltration and thus increases surface runoff and decreases groundwater recharge. Consequently, groundwater influence should be less important. Due to permafrost sealing of the ground, a much higher percentage of precipitation, regardless if related to rainfall or snowmelt runoff events, reaches the lake. Moreover, buffering of the lake level via groundwater is reduced for two reasons: (1) the groundwater level follows or at least responds to the global sea level and thus should be considerably deeper and (2) permafrost isolates the lake water body from groundwater influence although forming a talik. If both aspects are completely true, groundwater influence would have been eliminated by permafrost during the last glacial period. Then the typically high precipitation variability as observed in semiarid regions is not buffered any more by groundwater influence which consequently causes a much more direct link between precipitation, snowmelt and the lake level. Thus

Table 3
Correlated tephra layers with ages according to age-model 1 compared to ages from Stern (2008). Uncalibrated literature dates of 5022-2T1, 5022-2T24 and 5022-2T53 were recalibrated with CalPal and the CalPal_2007_HULU calibration curve. Dates of 5022-2T35, 5022-2T39 and 5022-2T52 are according to the age model of Haberzettl et al. (2009).

Tephra layer	Source volcano	Age model 1 (cal. ka BP)	Age (cal. ka BP)
5022-2T53	Hudson	8.40 ± 0.63	7.72 ± 0.14 Stern (2008)
5022-2T1	Mt. Burney	9.43 ± 0.72	9.44 ± 0.64 Stern (2008)
5022-2T24	Reclús	16.03 ± 0.56	15.12 ± 0.45 Stern (2008)
5022-2T35	(NAVZ)	44.53 ± 3.81	~34 Haberzettl et al. (2009)
5022-2T39	Mt. Burney	48.70 ± 4.95	~45 Haberzettl et al. (2009)
5022-2T52	Mt. Burney	50.87 ± 6.35	~54 Haberzettl et al. (2009)

Please cite this article in press as: Kliem, P., et al., Lithology, radiocarbon chronology and sedimentological interpretation of the lacustrine record from Laguna Potrok Aike, southern Patagonia, Quaternary Science Reviews (2012), http://dx.doi.org/10.1016/j.quascirev.2012.07.019

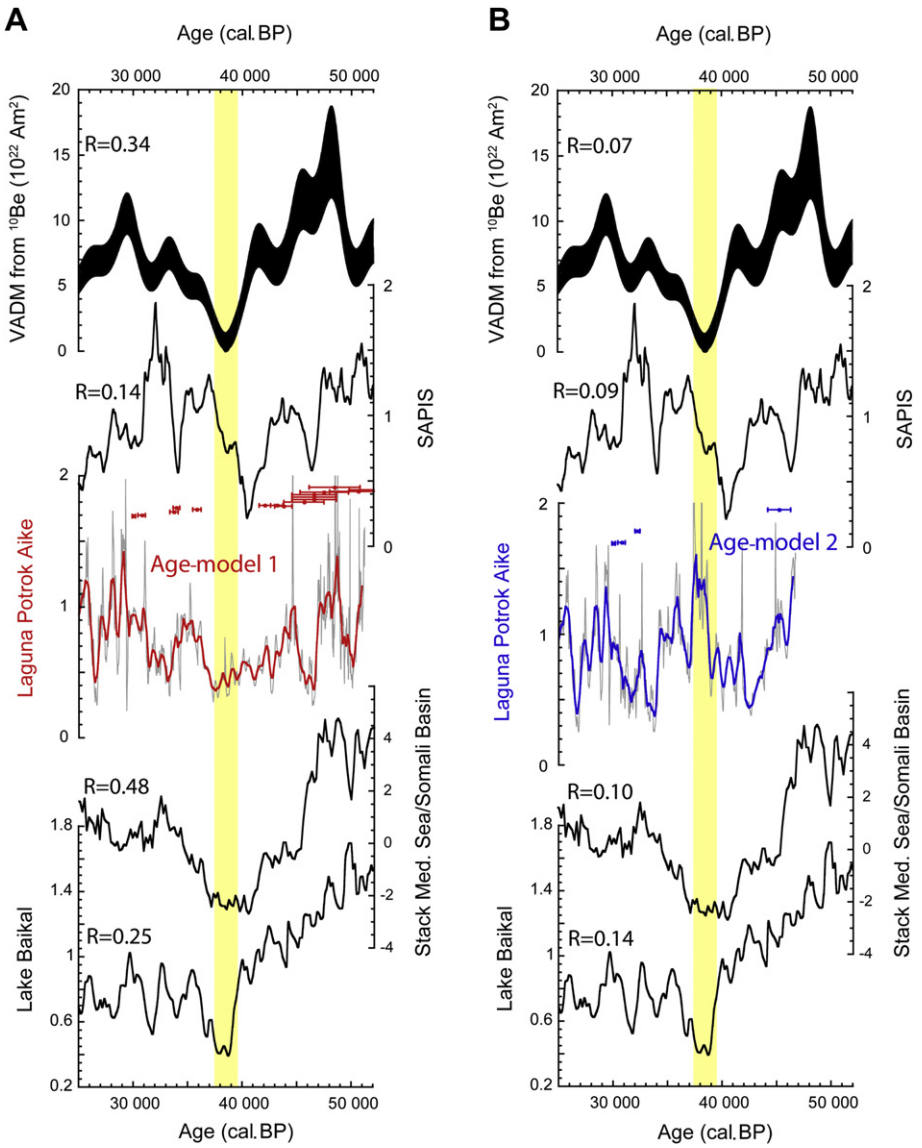

Fig. 11. Relative paleointensity proxy from Laguna Potrok Aike using A) Age-model 1 and B) Age-model 2 compared with independent geomagnetic field reconstructions from 55 to 25 cal. ka BP. From top to bottom: geomagnetic field intensity derived from the ^{10}Be-flux of the Summit ice core, Greenland (Muscheler et al., 2005), stack for the South Atlantic Ocean (SAPIS; Stoner et al., 2002), marine stack of the Mediterranean Sea and Somali Basin (Meynadier et al., 1992; Guyodo and Valet, 1996) and stack from Lake Baikal (Peck et al., 1996). Correlation coefficients are indicated. The shaded area indicates the geomagnetic Laschamp excursion at ca 38–39 cal. ka BP in the PASADO and ^{10}Be-derived records.

more pronounced lake level fluctuations can be expected under permafrost conditions. Moreover, a higher percentage of precipitation is transferred to the lake as infiltration is eliminated and also evaporation is less effective under the generally colder air temperatures of the glacial period. Relict permafrost features (sand-wedges) are actually widespread in southern Patagonia (Bockheim et al., 2009) and sand-wedges have also been detected in the catchment of Laguna Potrok Aike where they suggest permafrost conditions around 35 ka (Kliem et al., in this issue). The general decrease of mass movement deposits with time might also be related to a reduced subaquatic relief as the result of sediment accumulation and slope consolidation.

In addition to laminated pelagic sediments and mass movement deposits, tephra layers are the third dominant sediment feature. However, no tephras from local eruptions of the PAVF have been documented for the 51 ka record, although this volcanic area provides a huge source of volcaniclastic material and eruptions are ongoing until at least the early Holocene (Corbella, 2002). Since volcanic activities of the PAVF have developed toward the east, dominating west winds might have inhibited tephra accumulation from younger eruptions in Laguna Potrok Aike and only remote Andean tephras were recorded. Over- and underlain by lacustrine sediment, cohesionless tephra layers consisting of sorted silt may have acted as shear zones at the subaquatic slopes resulting in mass movements. This would explain that only one tephra layer exists between tephra layer t6–4 and t6–10 of PTA03/6 as the others probably have been eroded and are only preserved in the central deep site of 5022-2CP (Fig. 5). This also suggests unidentified hiatuses in PTA03/6 as no hiatus has been documented below 34 cal. ka BP (Haberzettl et al., 2009) which would explain that the proximal sedimentation rate at PTA03/6 is less than 1.0 mm/a compared to 0.6–2.4 mm/a in the profundal zone at 5022-2CP.

5.2. Chronology

The elaborated radiocarbon chronology (age-model 1) is hampered by several outliers representing ages considerably

Please cite this article in press as: Kliem, P., et al., Lithology, radiocarbon chronology and sedimentological interpretation of the lacustrine record from Laguna Potrok Aike, southern Patagonia, Quaternary Science Reviews (2012), http://dx.doi.org/10.1016/j.quascirev.2012.07.019

younger and older than the estimated age after the second iteration of the mixed-effect regression. Different reasons can be regarded as the cause for these results: stratigraphical mixing, hard-water and reservoir effects, variations in ^{14}C production (plateau effects) as well as contamination by modern carbon can theoretically influence radiocarbon dates (Cohen, 2003). Stratigraphical mixing caused e.g. by bioturbation or dating of roots as well as the hard-water effect can be excluded for this record. The observed concentration of aquatic moss fragments in certain sediment layers point to sedimentation events during which these mosses are transported from littoral to profundal zones of the lake (Fig. 6). Hence, it is not surprising that some dates from pelagic sediments vary toward higher ages indicating the dating of reworked material. Offsets to younger ages occur at the transition from lithological unit C-2 to C-1 until ca 30 cal. ka BP. These apparently too young dates might be explained by the sensibility of samples closer to the dating limit of the radiocarbon method for contamination by modern carbon (Olson and Eriksson, 1972). Contamination is known from fungi and bacterial activity as they assimilate modern CO_2 if stored for many years within sediment cores (Geyh et al., 1974) or under wet conditions after sampling (Wohlfarth et al., 1991). This explanation seems to be unlikely in our case as the cores were continuously stored under cool and dark conditions; samples were taken relatively fast after coring (10–12 months) and immediately dried after sampling. The most prominent too young dates (Poz-37075 with 34.4 cal. ka BP in 34.15 m cd-ec; Poz-32493 with 32.2 cal. ka BP in 33.88 m cd-ec) seem to be confirmed by the tephra layer 5022-2T35 if dated according to Haberzettl et al. (2009) and by one ^{230}Th-age dated to 29.4 ± 5.9 ka in 34.95 m cd-ec (Nuttin et al., in this issue) which question age-model 1. Considering these younger dates as true ages would imply a hiatus to the next older date of 10.1–12.3 ka. However, in the lithology no indication for such a large hiatus has been observed. Mass movements within that depth interval suggest some degree of erosion, but applying the mean event-corrected sedimentation rate of 0.9 mm/a a sediment package between ~9 and ~11 m would have to be eroded. This seems to be very unlikely for the profundal zone of the lake. Another option would be an unidentified hiatus related to desiccation. However, a permanent water column is suggested by continuous lacustrine sedimentation on the subaquatic terrace and by seismic results between ~30 and 53.5 ka (Gebhardt et al., 2012). Furthermore, the age of 5022-2T35 from Haberzettl et al. (2009) is questionable. Short term fluctuations of the atmospheric $^{14}C/^{12}C$ ratio caused by increased production of ^{14}C as a result of low paleomagnetic field intensity are another option to explain too young ages. Data available for calibrating ^{14}C ages vary up to 2000 years for the time window 30–50 cal. ka BP (Schramm et al., 2000) indicating short term fluctuations in atmospheric ^{14}C concentration. The two affected radiocarbon dates differ from the estimated age by ~11 ka and ~9 ka, respectively. It is conceivable that the short-living aquatic mosses might document fluctuations in the atmospheric $^{14}C/^{12}C$ ratio. Whether this is a realistic explanation and whether this effect is as large as ca 10 ka needs to be further investigated. At the older part of the record (>45 cal. ka BP) radiocarbon dates tend to show an asymptotic behavior, which can be a sign of underestimated ages close to the dating limit of the radiocarbon method (Chappell et al., 1996). Upcoming publications of high resolution radiocarbon dates for varve-dated sediments of Lake Suigetsu (Japan) might improve our understanding of the terrestrial radiocarbon calibration models and underlying ^{14}C variations back to the dating limit of this method (Nakagawa et al., 2012).

Age-model 2 as the conservative alternative for the age-depth modeling of sediments from Laguna Potrok Aike seems to be disproved by the two oldest tephra layers (Fig. 8B) and after comparison with global geomagnetic relative paleointensity data (Fig. 11). Therefore, we suggest following age-model 1 as the most likely chronology for the time being. Nevertheless, most radiocarbon dates approaching the limits of this dating method (30–45/50 ka BP) can be questioned and thus efforts have been undertaken to improve the reliability of our time control by additional and independent dating methods. As Ar/Ar dating of volcanic ashes turned out to be impossible due to the lack of suitable potassium feldspars (M. Storey, 2011; pers. comm.), our focus is now directed toward luminescence dating. Analyses of 38 samples from core 5022-1D have already been carried out and evaluated (Buylaert et al., in this issue). However, before these dates can be compared to the age models presented here, a thorough correlation between the composite profile from Site 2 (radiocarbon chronology and most other stratigraphic investigations) with Site 1 (luminescence dating) needs to be carried out.

5.3. Sedimentation rates

Calculated sedimentation rates for the sediment record range between 0.37 and 8.5 mm/a (mean: 2.07 mm/a). However, the percentage of mass movement deposits increases downcore but no erosion at their respective bases was assumed for the compilation of the event-corrected composite profile 5022-2CP and thus this effect is not reflected in the sedimentation rates. Sharp contacts to underlying sediments document some degree of erosion of pelagic sediments. Therefore, calculated sedimentation rates have to be regarded as minimum values as it is impossible to estimate the degree of erosion.

During three time periods sedimentation rates exceed 1 mm/a (Fig. 8C: 6.6–9.4 cal. ka BP, 23.7–31.1 cal. ka BP and 46.3–51.2 cal. ka BP). The first of these periods correlates with the transition from lithological unit B to A which is described as having the lowest lake level (33 m below the lake level of 2003) since the last glacial period due to dry conditions caused by strengthening of the Southern Hemispheric Westerlies (Haberzettl et al., 2007, 2008; Anselmetti et al., 2009). Profundal sedimentation increased probably because the lake level lowering exposed older terraces to erosion. Furthermore, a reduced water body would result in reduced accumulation space and therefore in increased sedimentation rates at the coring location. A more negative water balance of the lake between 9.2 and 8.7 cal. ka BP with considerable variations afterward is based on pollen and geochemical evidence (Mayr et al., 2007b).

If low lake levels at Laguna Potrok Aike cause higher sedimentation rates, increased sedimentation rates during the last glacial period centered around 27.4 and 48.8 cal. ka BP may also document lower lake levels. For the younger glacial period with higher sedimentation rates from 31.1 to 23.7 cal. ka BP it would be plausible to assume that at the begin of the LGM a general decrease in precipitation occurred which might have caused a lake level lowering with enforced erosion of the then exposed former littoral zone. However, this assumption needs to be verified by additional future studies. In contrast, the record from PTA03/6 documents a higher lake level between 45 and 51 cal. ka BP (Haberzettl et al., 2009). This is much higher than the modern water level and supported by IRSL dating of tephra layers now exposed at terrace-outcrops that have been deposited in the lake between 44 and 48 ka suggesting overflow conditions (Kliem et al., in this issue). Based on this data, the hypothesis that higher sedimentation rates are linked to lake level low stands has either to be falsified or the temporal lake level variability was much higher than anticipated.

5.4. Formation of the lake basin

The expected base of lacustrine sediments inferred by a seismic survey is in 370 m blf (below lake floor which is presently at 13 m

Please cite this article in press as: Kliem, P., et al., Lithology, radiocarbon chronology and sedimentological interpretation of the lacustrine record from Laguna Potrok Aike, southern Patagonia, Quaternary Science Reviews (2012), http://dx.doi.org/10.1016/j.quascirev.2012.07.019

a.s.l.) (Gebhardt et al., 2011). Considering an overall mean sedimentation rate of 2.07 mm/a for the entire history of Laguna Potrok Aike, the start of lacustrine sedimentation can be estimated to ~180 ka. This represents also the approximate date of the maar eruption as the crater bottom filled-up rapidly with groundwater after the eruption. However, this date contradicts the Ar/Ar date of 770 ± 240 ka for a basaltic clast from the phreatomagmatic tephra of the maar eruption (Zolitschka et al., 2006). Explanations for this discrepancy could be unreliable dating or frequent desiccations of the lake basin which introduce periods without sedimentation and sediment removal by deflation as observed for this region today, e.g. for Laguna Maar Bismarck (Gebhardt et al., 2012). Indeed, stacked sand dunes approximately 200 m below the present lake level in the eastern part of the lake basin, i.e. older than 51.2 cal. ka BP, have been inferred by seismic data and support desiccation and deflation just prior to the start of the sedimentary record discussed here (Gebhardt et al., 2012). So far, no desiccation hiatus was identified lithologically. However, mass movements might have eroded such features at the coring location. Although high lake levels are documented for this record, low lake levels have not been determined prior to the Lateglacial. Furthermore, the presence of aquatic mosses throughout 5022-2CP supports at least ephemeral water bodies for the last 51.2 cal. ka BP confirming that no desiccation occurred during this time interval. But periods of desiccation accompanied by wind erosion most likely existed before (Gebhardt et al., 2012) reducing the total amount of accumulated sediment and thus bringing the extrapolated age for the bedrock to sediment transition (using the mean sedimentation rate) and the Ar/Ar date for the maar formation into agreement.

6. Conclusions and outlook

The Holocene and the glacial periods of the 106.09 m long composite profile from Site 2 (5022-2CP) of Laguna Potrok Aike can be distinguished by dominance of laminated silts and the occurrence of carbonate crystals during the Holocene and by laminated silts intercalated with fine sand and coarse silt layers as well as mass movement deposits during the last glacial. The transition is characterized by a high content of plant macro remains, that started abruptly at 17.2 ± 0.5 cal. ka BP and continued until 12.2 ± 0.7 cal. ka BP. This period correlates with the first and second major deglacial warming step known from marine and Antarctic ice core climate records. Mass movement deposits are important for the sedimentation history of the lake basin as they comprise over 50% of the record and increase downward in frequency. Rapid and frequent lake level changes might have enforced the collapse of slopes during the glacial period which increased the occurrence of mass movement deposits. Their general decrease with time is probably the effect of decreasing sub-aquatic relief energy, slope consolidation and a less inclined slope angle during basin development.

Prevailing permafrost conditions and a decreased sea level decoupled the lake water body from groundwater which made the lake level more susceptible to variations in precipitation. Moreover, frozen ground inhibited infiltration. Together, these permafrost-related factors increased not only the amplitude but also the frequency of glacial lake level fluctuations.

The complete record was datable with the radiocarbon method. Sufficient amounts of carbon were found in layers containing organic macro remains. In most cases stems of aquatic mosses were analyzed, which apparently grew throughout the record. For age-depth modeling, an event-corrected composite profile of 45.80 m cd-ec was developed using the mixed-effect regression procedure. Two age-depth models consider two different interpretations of the same data and have been validated with tephra correlations and geomagnetic relative paleointensity records. For the favored age-model 1 several outliers of significantly older and younger ages have been removed. The age-model 2 includes ages strictly according to the law of superposition. However and based on a comparison of both models with the global geomagnetic relative paleointensity and tephrochronological data, age-model 1 is preferred.

Applying age-model 1, the bottom age of the record was dated to 51.2 cal. ka BP. Throughout this time range the lake basin was permanently filled with water; the water column distinctly exceeded modern water depth between 45 and 51 cal. ka BP and around 17 cal. ka BP (Kliem et al., in this issue) and was much lower between 9.4 and 7.3 cal. ka BP (Anselmetti et al., 2009). Considering the Ar/Ar age of the maar eruption and the extrapolation of sedimentation rates to the lacustrine base inferred by seismic data, the lake basin should be completely filled with sediment. Most likely, persistent desiccations causing erosion or at least no sedimentation have to have existed before 51.2 cal. ka BP to explain this discrepancy.

Acknowledgments

This research is supported by the International Continental Scientific Drilling Program (ICDP) in the framework of the “Potrok Aike Maar Lake Sediment Archive Drilling Project” (PASADO). Funding for drilling was provided by the ICDP, the German Science Foundation (DFG ZO 102/11-1,2), the Swiss National Funds (SNF), the Natural Sciences and Engineering Research Council of Canada (NSERC), the Swedish Vetenskapsradet (VR) and the University of Bremen.

References

Anselmetti, F.S., Ariztegui, D., De Batist, M., Gebhardt, A.C., Haberzettl, T., Niessen, F., Ohlendorf, C., Zolitschka, B., 2009. Environmental history of southern Patagonia unravelled by the seismic stratigraphy of Laguna Potrok Aike. Sedimentology 56, 873–892.

Baruth, B., Endlicher, W., Hoppe, P., 1998. Climate and desertification processes in Patagonia. Bamberger Geographische Schriften 15, 307–320.

Bertrand, S., Charlet, F., Chapron, E., Fagel, N., De Batist, M., 2008. Reconstruction of the Holocene seismotectonic activity of the southern Andes from seismites recorded in Lago Icalma, Chile, 39°S. Palaeogeography, Palaeoclimatology, Palaeoecology 259, 301–322.

Bockheim, J., Coronato, A., Rabassa, J., Ercolano, B., Ponce, J., 2009. Relict sand wedges in southern Patagonia and their stratigraphic and paleo-environmental significance. Quaternary Science Reviews 28, 1188–1199.

Buylaert, J.P., Murray, A.S., Gebhardt, C., Sohbati, R., Ohlendorf, C., Thiel, C., Zolitschka, B. Luminescence dating of the PASADO core 5022-1D from Laguna Potrok Aike (Argentina) using IRSL signals from feldspar. Quaternary Science Reviews, in this issue.

Caldenius, C., 1932. Las glaciaciones cuarternarias en la Patagonia y Tierra del Fuego. Geografisker Annaler 22, 1–164.

Chappell, J., Head, J., Magee, J., 1996. Beyond the radiocarbon limit in Australian archeology and Quaternary research. Antiquity 70, 543–552.

Cohen, A.S., 2003. Paleolimnology. The History and Evolution of Lake Systems. Oxford University Press, Oxford.

Conze, R., Wallrabe-Adams, H., Graham, C., Krysiak, F., 2007. Joint data management in ICDP projects and IODP mission specific platform expeditions. Scientific Drilling 4, 32–34.

Corbella, H., 2002. El campo volcano-tectónico de Pali Aike. In: Haller, M. (Ed.), Geología y Recursos Naturales de Santa Cruz. Asociación Geológica Argentina, pp. 285–302. Buenos Aires.

Coronato, A., Ercolano, B., Corbella, H., Tiberi, P. Glacial, fluvial and volcanic landscape evolution in the Laguna Potrok Aike maar area, southernmost Patagonia, Argentina, in this issue.

Frey, K.E., Smith, L.C., 2005. Amplified carbon release from vast West Siberian peatlands by 2100. Geophysical Research Letters 32.

Gebhardt, A.C., De Batist, M., Niessen, F., Anselmetti, F.S., Ariztegui, D., Haberzettl, T., Kopsch, C., Ohlendorf, C., Zolitschka, B., 2011. Deciphering lake and maar geometries from seismic refraction and reflection surveys in Laguna Potrok Aike (southern Patagonia, Argentina). Journal of Volcanology and Geothermal Research 201, 357–363.

Gebhardt, A.C., Ohlendorf, C., Niessen, F., De Batist, M., Anselmetti, F.S., Ariztegui, D., Kliem, P., Wastegård, S., Zolitschka, B., 2012. Seismic evidence of up to 200 m lake level change in southern Patagonia since MIS4. Sedimentology 59, 1087–1100.

Geyh, M.A., Krumbein, W.E., Kudrass, H.-R., 1974. Unreliable 14C dating of long-stored deep-sea sediments due to bacterial activity. Marine Geology 17, 45–50.
Gilli, A., Ariztegui, D., Anselmetti, F.S., McKenzie, J.A., Markgraf, V., Hajdas, I., McCulloch, R.D., 2005. Mid-Holocene strengthening of the southern westerlies in South America – sedimentological evidences from Lago Cardiel, Argentina (49°S). Global and Planetary Change 49, 75–93.
Girardclos, S., Schmidt, O.T., Sturm, M., Ariztegui, D., Pugin, A., Anselmetti, F.S., 2007. The 1996 AD delta collapse and large turbidite in Lake Brienz. Marine Geology 241.
Guillou, H., Singer, B.S., Laj, C., Kissel, C., Scaillet, S., Jicha, B.R., 2004. On the age of the Laschamp geomagnetic excursion. Earth and Planetary Science Letters 227, 331.
Guyodo, Y., Valet, J.-P., 1996. Relative variations in geomagnetic intensity from sedimentary records: the past 200,000 years. Earth and Planetary Science Letters 143, 23–36.
Haberzettl, T., Fey, M., Lücke, A., Maidana, N., Mayr, C., Ohlendorf, C., Schäbitz, F., Schleser, G.H., Wille, M., Zolitschka, B., 2005. Climatically induced lake level changes during the last two millennia as reflected in sediments of Laguna Potrok Aike, southern Patagonia (Santa Cruz, Argentina). Journal of Paleolimnology 33, 283–302.
Haberzettl, T., Corbella, H., Fey, M., Janssen, S., Lücke, A., Mayr, C., Ohlendorf, C., Schäbitz, F., Schleser, G.H., Wille, M., Wulf, S., Zolitschka, B., 2007. Lateglacial and Holocene wet-dry cycles in southern Patagonia: chronology, sedimentology and geochemistry of a lacustrine record from Laguna Potrok Aike, Argentina. The Holocene 17, 297–310.
Haberzettl, T., Kück, B., Wulf, S., Anselmetti, F., Ariztegui, D., Corbella, H., Fey, M., Janssen, S., Lücke, A., Mayr, C., Ohlendorf, C., Schäbitz, F., Schleser, G.H., Wille, M., Zolitschka, B., 2008. Hydrological variability in southeastern Patagonia and explosive volcanic activity in the southern Andean Cordillera during Oxygen Isotope Stage 3 and the Holocene inferred from lake sediments of Laguna Potrok Aike, Argentina. Palaeogeography, Palaeoclimatology, Palaeoecology 259, 213–229.
Haberzettl, T., Anselmetti, F.S., Bowen, S.W., Fey, M., Mayr, C., Zolitschka, B., Ariztegui, D., Mauz, B., Ohlendorf, C., Kastner, S., Lücke, A., Schäbitz, F., Wille, M., 2009. Late Pleistocene dust deposition in the Patagonian steppe – extending and refining the paleoenvironmental and tephrochronological record from Laguna Potrok Aike back to 55 ka. Quaternary Science Reviews 28, 2927–2939.
Hahn, A., Kliem, P., Ohlendorf, C., Zolitschka, B., Rosen, P. Climate induced changes in the content of carbonaceous and organic matter of sediments from Laguna Potrok Aike (Argentina) during the past 50 ka inferred from infrared spectroscopy. Quaternary Science Reviews, in this issue.
Hampton, M.A., Lee, H.J., Locat, J., 1996. Submarine landslides. Reviews of Geophysics 34, 33–59.
Heegaard, E., Birks, H.J.B., Telford, R.J., 2005. Relationships between calibrated ages and depth in stratigraphical sequences: an estimation procedure by mixed-effect regression. The Holocene 15, 612–618.
Hein, A.S., Hulton, N.R.J., Dunai, T.J., Sudgen, D.E., Kaplan, M.R., Xu, S., 2010. The chronology of the Last Glacial Maximum and deglacial events in central Argentine Patagonia. Quaternary Science Reviews 29, 1212–1227.
Hughen, K.A., 2007. Radiocarbon dating of deep-sea sediment. In: Hillaire-Marcel, de Vernal, A. (Eds.), Proxies in Late Cenozoic Paleoceanography. Elsevier, pp. 99–138.
Jouve, G., Francus, P., Lamoureux, S., Provencher-Nolet, L., Hahn, A., Haberzettl, T., Fortin, D., Nuttin, L. Microsedimentological characterization using image analysis and XRF as indicators of sedimentary processes and climate changes during Late Glacial at Laguna Potrok Aike, Santa Cruz, Argentina. Quaternary Science Reviews, in this issue.
Kilian, R., Hohner, M., Biester, H., Wallrabe-Adams, H.J., Stern, C.R., 2003. Holocene peat and lake sediment tephra record from the southernmost Chilean Andes (53–55°S). Revista Geológica de Chile 30, 23–37.
Kliem, P., Buylaert, J.P., Hahn, A., Mayr, C., Murray, A.S., Ohlendorf, C., Veres, D., Wastegård, S., Zolitschka, B. Magnitude, Geomorphologic Response and Climate Links of Lake Level Oscillations at Laguna Potrok Aike, Patagonian Steppe, Argentina, in this issue.
Kokfelt, U., Rosén, P., Schoning, K., Christensen, T.R., Förster, J., Karlsson, J., Reuss, N., Rundgren, M., Callaghan, T.V., Jonasson, C., Hammarlund, D., 2009. Ecosystem responses to increased precipitation and permafrost decay in subarctic Sweden inferred from peat and lake sediments. Global Change Biology 15, 1652–1663.
Lamy, F., Kaiser, J., Arz, H.W., Hebbeln, D., Ninnemann, U., Timm, O., Timmermann, A., Toggweiler, J.R., 2007. Modulation of the bipolar seesaw in the Southeast Pacific during termination 1. Earth and Planetary Science Letters 259, 400–413.
Lisé-Pronovost, A., St-Onge, G., Gogorza, C., Zolitschka, B. High-resolution paleomagnetic secular variation and relative paleointensity since the Late Pleistocene and Southern South America. Quaternary Science Reviews, in this issue.
Locat, J., Lee, H.J., 2002. Submarine landslides: advances and challenges. Canadian Geotechnical Journal 39, 193–212.
Markgraf, V., Whitlock, C., Haberle, S., 2007. Vegetation and fire history during the last 18,000 cal yr B.P. in southern Patagonia: Mallin Pollux, Coyhaique, Province Aisen. Palaeogeography, Palaeoclimatology, Palaeoecology 254, 492–507.
Markgraf, V., Huber, U.M., 2010. Late and postglacial vegetation and fire history in southern Patagonia and Tierra del Fuego. Palaeogeography, Palaeoclimatology, Palaeoecology 297, 351–366.
Mayr, C., Lücke, A., Stichler, W., Trimborn, P., Ercolano, B., Oliva, G., Ohlendorf, C., Soto, J., Fey, M., Haberzettl, T., Janssen, S., Schäbitz, F., Schleser, G.H., Wille, M., Zolitschka, B., 2007a. Precipitation origin and evaporation of lakes in semi-arid Patagonia (Argentina) inferred from stable isotopes ($\delta^{18}O$, $\delta^{2}H$). Journal of Hydrology 334, 53–63.
Mayr, C., Wille, M., Haberzettl, T., Fey, M., Janssen, S., Lücke, A., Ohlendorf, C., Oliva, G., Schäbitz, F., Schleser, G.H., Zolitschka, B., 2007b. Holocene variability of the southern hemisphere westerlies in Argentinean Patagonia (52°S). Quaternary Science Reviews 26, 579–584.
Mayr, C., Lücke, A., Maidana, N.I., Wille, M., Haberzettl, T., Corbella, H., Ohlendorf, C., Schäbitz, F., Fey, M., Janssen, S., Zolitschka, B., 2009. Isotopic fingerprints on lacustrine organic matter from Laguna Potrok Aike (southern Patagonia, Argentina) reflect environmental changes during the last 16,000 years. Journal of Paleolimnology 42, 81–102.
Mazzarini, F., D'Orazio, M., 2003. Spatial distribution of cones and satellite-detected lineaments in the Pali Aike Volcanic Field (southernmost Patagonia): insights into the tectonic setting of a Neogene rift system. Journal of Volcanology & Geothermal Research 125, 291–305.
McCulloch, R.D., Fogwill, C.J., Sugden, D.E., Bentley, M.J., Kubik, P.W., 2005. Chronology of the Last Glaciation in Central Strait of Magellan and Bahía Inútil, southernmost South America. Geografiska Annaler, Series A: Physical Geography 87, 289–312.
Meglioli, A. 1992. Glacial Geology and Geochronology of Southernmost Patagonia and Tierra del Fuego, Argentina and Chile. Ph.D. dissertation, Leigh University, Bethlehem PA, U.S.A., 216 pp.
Mercer, J.H., 1976. Glacial history of southernmost South America. Quaternary Research 6, 125–166.
Meyer, I., Wagner, S., 2008. The Little Ice Age in southern Patagonia: comparison between paleoecological reconstructions and downscaled model output of a GCM simulation. PAGES News 16, 12–13.
Meynadier, L., Valet, J.-P., Weeks, R., Shackleton, N.J., Hagee, V.L., 1992. Relative geomagnetic intensity of the field during the last 140 ka. Earth and Planetary Science Letters 114, 39–57.
Moy, C.M., Dunbar, R.B., Guilderson, T.P., Waldmann, N., 2011. A geochemical and sedimentary record of high southern latitude Holocene climate evolution from Lago Fagnano, Tierra del Fuego. Earth and Planetary Science Letters 302, 1–13.
Muscheler, R., Beer, J., Kubik, P.W., Synal, H.-A., 2005. Geomagnetic field intensity during the last 60,000 years based on ^{10}Be and ^{36}Cl from the summit ice cores and ^{14}C. Quaternary Science Reviews 24, 1849–1860.
Myrbo, A. 2007. Smear Slide Identifications: the Practical Basics. Limnological Research Center Core Facility, SOP Series, Draft v. 3.1; Downloaded on 3.11.2010 from www.lrc.geo.umn.edu.
Nakagawa, T., Gotanda, K., Haraguchi, T., Danhara, T., Yonenobu, H., Brauer, A., Yokoyama, Y., Tada, R., Takemura, K., Staff, R.A., Payne, R., Ramsey, C.B., Bryant, C., Brock, F., Schlolaut, G., Marshall, M., Tarasov, P., Lamb, H., 2012. SG06, a fully continuous and varved sediment core from Lake Suigetsu, Japan: stratigraphy and potential for improving the radiocarbon calibration model and understanding of late Quaternary climate changes. Quaternary Science Reviews 36, 164–176.
Nuttin, L., Francus, P., Preda, M., Ghaleb, B., Hillaire-Marcel, C. Authigenic, detrital and diagenetic minerals in the Laguna Potrok Aike sedimentary sequence. Quaternary Science Reviews, in this issue.
Ohlendorf, C., Gebhardt, C., Hahn, A., Kliem, P., Zolitschka, B., 2011. The PASADO core processing strategy – a proposed new protocol for sediment core treatment in multidisciplinary lake drilling projects. Sedimentary Geology 239, 104–115.
Olson, I.U., Eriksson, K.G., 1972. Fractionation studies of the shell of foraminifera. Etudes sur la Quaternaire dans le Monde, 921–923.
Peck, J.A., King, J.W., Colman, S.M., Kravchinsky, V.A., 1996. An 84-kyr paleomagnetic record from the sediments of Lake Baikal, Siberia. Journal of Geophysical Research 101 (B5), 11,365–11,385.
Rabassa, J., Clapperton, C.M., 1990. Quaternary glaciations of the southern Andes. Quaternary Science Reviews 9, 153–174.
Schnurrenberger, D., Russell, J., Kelts, K., 2003. Classification of lacustrine sediments based on sedimentary components. Journal of Paleolimnology 29, 141–154.
Schramm, A., Stein, M., Goldstein, S.L., 2000. Calibration of the ^{14}C time scale to >40 ka by ^{234}U-^{230}Th dating of Lake Lisan sediments (Last Glacial Dead Sea). Earth and Planetary Science Letters 175, 27–40.
Stern, C.R., 2008. Holocene tephrochronology record of large explosive eruptions in the southernmost Patagonian Andes. Bulletin of Volcanology 70, 435–454.
Stoner, J.S., Laj, C., Channell, J.E.T., Kissel, C., 2002. South Atlantic and North Atlantic geomagnetic paleointensity stacks (0–80 ka): implications for inter-hemispheric correlation. Quaternary Science Reviews 21, 1141–1151.
Strasser, M., Stegmann, S., Bussmann, F., Anselmetti, F.S., Rick, B., Kopf, A., 2007. Quantifying subaqueous slope stability during seismic shaking: lake Lucerne as model for ocean margins. Marine Geology 240, 77–97.
Sturm, M., Siegenthaler, C., Pickrill, R.A., 1995. Turbidites and 'Homogenites'. A Conceptual Model of Flood and Slide Deposits. 5ème congrès de Sédimentologie. ASF. Livre des Résumés 22.
Sultan, N., Cochonat, P., Canals, M., Cattaneo, A., Dennielou, B., Haflidason, H., Laberg, J.S., Long, D., Mienert, J., 2004. Triggering mechanisms of slope instability processes and sediment failures on continental margins: a geotechnical approach. Marine Geology 213, 291–321.
Uliana, M.A., Biddle, T., 1988. Mesozoic-Cenozoic paleogeographic and geodynamic evolution of southern South America. Revista Brasileira de Geosciencas 18, 172–190.
Wagner, S., Widmann, M., Jones, J., Haberzettl, T., Lücke, A., Mayr, C., Ohlendorf, C., Schäbitz, F., Zolitschka, B., 2007. Transient simulations, empirical reconstructions and forcing mechanisms for the Mid-Holocene hydrological climate in southern Patagonia. Climate Dynamics 29, 333–355.

Please cite this article in press as: Kliem, P., et al., Lithology, radiocarbon chronology and sedimentological interpretation of the lacustrine record from Laguna Potrok Aike, southern Patagonia, Quaternary Science Reviews (2012), http://dx.doi.org/10.1016/j.quascirev.2012.07.019

Wastegård, S., Veres, D., Kliem, P., Ohlendorf, C., Zolitschka, B. Towards a late Quaternary tephrochronological framework for the southernmost part of South America – the Laguna Potrok Aike tephra record. Quaternary Science Reviews, in this issue.

Weischet, W., 1996. Regionale Klimatologie. Teil 1: Die Neue Welt: Amerika, Neuseeland, Australien. Teubner, Stuttgart.

Weninger, B., Jöris, O., 2008. A 14C age calibration curve for the last 60 ka: the Greenland-Hulu U/Th timescale and its impact on understanding the Middle to Upper Paleolithic transition in Western Eurasia. Journal of Human Evolution 55, 772–781.

Weninger, B., Jöris, O., Danzeglocke, U., 2010. CalPal-2007. Cologne Radiocarbon Calibration & Palaeoclimate Research Package. http://www.calpal.de/ (accessed 25.05.10.).

Wille, M., Schäbitz, F., 2009. Late-glacial and Holocene climate dynamics at the steppe/forest ecotone in southernmost Patagonia, Argentina: the pollen record from a fen near Brazo Sur, Lago Argentino. Vegetation History and Archaeobotany 18, 225–234.

Wohlfarth, B., Skog, G., Possnert, G., Holmquist, B., 1991. Pitfalls in the AMS radiocarbon-dating of terrestrial macrofossils. Journal of Quaternary Science 13, 137–145.

Zolitschka, B., Schäbitz, F., Lücke, A., Corbella, H., Ercolano, B., Fey, M., Haberzettl, T., Janssen, S., Maidana, N., Mayr, C., Ohlendorf, C., Oliva, G., Paez, M.M., Schleser, G.H., Soto, J., Tiberi, P., Wille, M., 2006. Crater lakes of the Pali Aike Volcanic Field as key sites for paleoclimatic and paleoecological reconstructions in southern Patagonia, Argentina. Journal of South American Earth Sciences 21, 294–309.

Please cite this article in press as: Kliem, P., et al., Lithology, radiocarbon chronology and sedimentological interpretation of the lacustrine record from Laguna Potrok Aike, southern Patagonia, Quaternary Science Reviews (2012), http://dx.doi.org/10.1016/j.quascirev.2012.07.019